ANGELHY

Innovative solutions for design and strengthening of telecommunications and transmission lattice towers using large angles from high strength steel and hybrid techniques of angles with FRP strips

WORK PACKAGE 4 – DELIVERABLE 4.4

Design guide and recommendations

Coordinator:

National Technical University of Athens - NTUA, Greece

Beneficiaries:

ArcelorMittal Belval & Differdange SA - AMBD, Luxembourg

Université de Liège - ULG, Belgium

COSMOTE Kinites Tilepikoinonies AE - COSMOTE, Greece

Centre Technique Industriel de la Construction Metallique - CTICM, France

SIKA France SAS - SIKA, France

AUTHORS:

ArcelorMittal Belval & Differdange SA – AMBD, Luxembourg
Global R&D
66, rue de Luxembourg
Esch-sur-Alzette
Author: Mike Tibolt

CENTRE TECHNIQUE INDUSTRIEL DE LA CONSTRUCTION METALLIQUE - CTICM
Steel Construction Research Division
Espace Technologique – Immeuble Apollo
L'Orme des Merisiers – F-91193 Saint Aubin
Authors: André Beyer, Alain Bureau

NATIONAL TECHNICAL UNIVERSITY OF ATHENS
Institute of Steel Structures
Iroon Polytechniou 9, 15780 Athens, Greece
Authors: Ioannis Vayas, Konstantinos Vlachakis

SIKA France SAS
84 rue Edouard Vaillant, 93350 Le Bourget, France
Authors: Yvon Giquel, Sébastien Reygner

UNIVERSITE DE LIEGE
Faculty of Applied Sciences, ArGEnCo Department
Quartier Polytech 1, Allée de la Découverte, 9, B52/3, 4000 Liège, Belgium
Authors: Marios-Zois Bezas, Jean-Pierre Jaspart, Jean-François Demonceau

Table of Contents

1 Scope

The present document gives basic design rules and recommendations for section and member verification of hot-rolled steel angle profiles, hot-rolled steel angle profiles strengthened externally or externally and internally with CFRP-strips and of closely built-up angle members for the application in steel lattice towers.

The present rules apply to hot-rolled equal leg angles according to EN 10056-1: 2017 and built-up sections made of equal and unequal cross-sections and bolted packing plates.

The design guide applies steel grades as listed in EN 1993-1-1 up to and including S460.

The CFRP-strips are made of Sika CarboDur S and the application of the strips should follow the procedure defined by the producer.

Fatigue design of angles members is not subject of the present design guide.

2   Notations, symbols and abbreviations

2.1   Conventions for member axes for single angles

The notations for the geometrical, material and other properties follow those given in prEN 1993-1-1 [1]. Figure 2-1 illustrates the notation for the geometrical properties, the geometrical axes as well as the principal axes.

G	centre of gravity
h,t	geometrical properties (c=h-t-r)
u-u	major principal axis or weak axis
v-v	minor principal axis or strong axis
y,z	geometrical axes
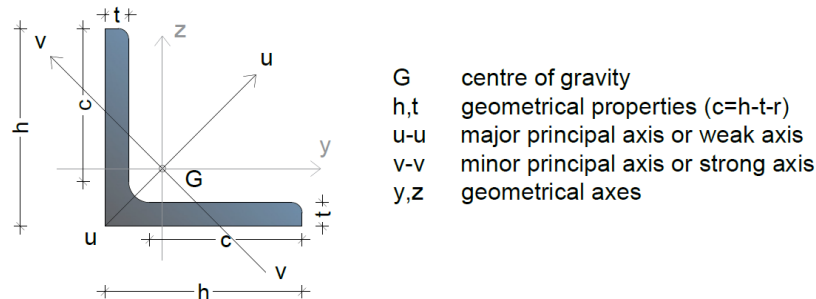
Figure 2-1 : Notations for geometrical properties and principal axes for single angle

(1) The convention for member axes is:

x-x – along the member

y-y – axis of the cross-section

z-z – axis of the cross-section

(2) For steel members, the conventions used for angle sections axes are:

y-y – cross-section axis parallel to the smaller leg

z-z – cross-section axis perpendicular to the smaller leg

u-u – major principal axis

v-v – minor principal axis

2.2   Symbols

A	cross-sectional area
A_{eff}	effective area of a cross-section
A_f	cross-sectional area of CFRP plates
A_{net}	net area of a cross-section
E_f	modulus of elasticity of CFRP material
E_s	modulus of elasticity of steel material
f_f	tensile strength of CFRP material
$f_{f,nom}$	nominal tensile strength of CFRP material
f_y	yield limit of steel material
f_u	tensile strength of steel material
I_{eff}	effective moment of inertia
I_u, I_v	moment of inertia about u-u axis and v-v axis, respectively
I_y, I_z	moment of inertia about y-y axis and z-z axis, respectively
L_{cr}	buckling length
$M_{b,Rd}$	design value of the buckling resistance of a member in bending
$M_{pl,Rd}$	design value of the plastic moment resistance
M_{Rk}	characteristic value of the resistance to bending moment
$M_{y,Rk}$	characteristic value of the resistance to bending moment about y-y axis
$M_{z,Ed}$	design value of the bending moment about z-z axis
$M_{z,Rd}$	design value of the resistance to bending moment about z-z axis
$M_{z,Rk}$	characteristic value of the resistance to bending moment about z-z axis
$N_{b,Rd}$	design syalue of the buckling resistance of a member in compression
$N_{c,Rd}$	design value of the resistance to axial force of the cross-section for uniform

N_{cr}	elastic critical axial force for the relevant buckling mode based on the gross cross-sectional properties
$N_{cr,T}$	elastic critical axial force for torsional buckling
$N_{cr,TF}$	elastic critical axial force for torsional-flexural buckling
$N_{cr,y}$, $N_{cr,z}$	elastic critical axial force for flexural buckling about y-y axis and z-z axis, respectively
N_{Rd}	design value of the resistance to axial force N_{Rk} characteristic value of the resistance to axial force
$N_{t,Rd}$	design value of the resistance to tension axial force
u_{Gs}	distance of centroid from heel in u direction
W_{eff}	effective section modulus
$W_{eff,min}$	minimum effective section modulus
$W_{el,u}$, $W_{el,v}$	elastic section modulus for bending about u-u axis and v-v axis, respectively
$W_{pl,u}$, $W_{pl,v}$	plastic section modulus for bending about u-u axis and v-v axis, respectively
y_{Gs}	distance of centroid from heel in y-direction
z_{Gs}	distance of centroid from heel in z-direction
h	width of a cross-section
c	width or depth of a part of a cross-section (c=h-t-r)
fy	yield strength
i	radius of gyration about the relevant axis, determined using the properties of the gross cross-section
i_y, i_z	radius of gyration for bending about y-y axis and z-z axis respectively
k_σ	plate buckling factor
r	radius of root fillet
t	thickness of a cross-section
Φ	value to determine the reduction factor χ for flexural buckling
Φ_{LT}	value to determine the reduction factor χ_{LT} for lateral torsional buckling
α	imperfection factor
α_{LT}	imperfection factor for lateral torsional buckling
γ_{M0}	partial factor for resistance of cross-sections
γ_{M1}	partial factor for resistance of members to instability assessed by member checks
λ	relative slenderness for flexural buckling
λ_{LT}	relative slenderness for lateral torsional buckling
η	modular ratio between steel and FRP material
χ_{LT}	reduction factor for lateral torsional buckling
χ_u	reduction factor due to flexural buckling about u-u axis
χ_v	reduction factor due to flexural buckling about v-v axis
ψ	ratio of end moments in a segment of beam, or stress ratio

3   Angle profiles

Hot-rolled equal leg and unequal leg angles profiles for steel lattice towers are typically available in a range from L45x45 to L300x300 resp. from L120x80 to L250x90. The thickness range varies from 4 mm to 35 mm for the equal leg profiles and from 8mm to 16mm for the unequal leg profiles.

Hot-rolled equal leg and unequal leg angles are available in steel grades as indicated in Table 3-1.

Table 3-1: Steel grades for hot-rolled angle profiles

S235	S355					S460
JR/J0/J2/K2	JR/J0/J2/K2	M	ML	J0W/J2W/K2W	G4/G11/G12+M*	M

* Off-shore grades.

In steel lattice towers, single equal and unequal angle profiles are used for the main (e.g. legs), the primary and secondary bracing members (e.g. diagonals) of the tower.

In case the load bearing resistance of single angle members is insufficient, it is possible to connect the angles in a back-to-back or a star-battened configuration (see Figure 3-1). The connection between the profiles is realized with bolted or welded packing plates.
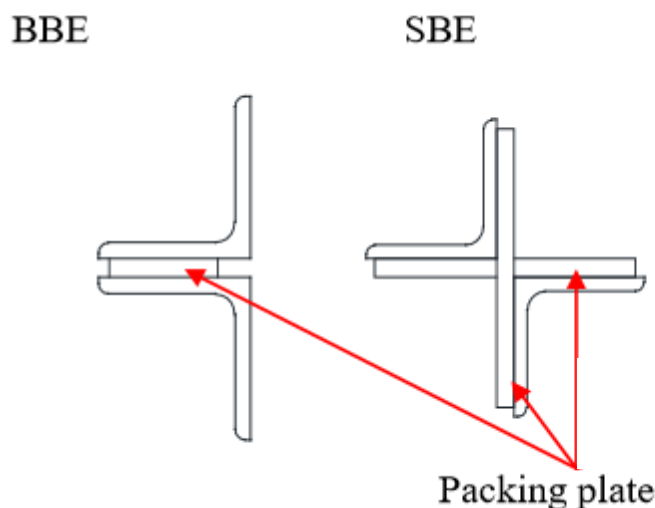
Figure 3-1: Back-to-back configuration (left) and star battened configuration (right)

According to [1], closely-built up members can be considered as one single integral member ignoring the shear stiffness if the conditions in Table 3-2 are met. Otherwise, the shear stiffness should be considered.

Table 3-2: Maximum spacing for interconnections in closely spaced built-up or star battened angle members

Type of built-up members	Maximum spacing between interconnections[a]
Members connected by bolts or welds	$15i_{min}$
Members connected by pair of battens	$70i_{min}$
[a] Centre-tocentre distance of interconnections i_{min} is the minimum radius of gyration of one chord or angle.	

The rules in [1] are valid for closely built-up members fabricated from identic angle profiles. The present design guide also gives rules for built-up members with unequal angle sections in chapter 10.

4 CFRP-material

The Sika CarboDur system is a high-performance structural strengthening system designed and used for strengthening concrete, timber, masonry and steel structures in post construction.

It is used to improve or increase the performance and resistance of structures for increased load capacity, improvement of serviceability and durability or resistance to possible events (earthquakes, impact or explosion etc…).

The system is consisting of Sika CarboDur plates and Sikadur 30 adhesive.

Sika CarboDur plates are pultruded carbon fibre reinforced polymer (CFRP) laminates, available in several widths (from 5 to 15cm). They are bonded onto the structure as externally bonded reinforcement using Sikadur 30 epoxy resin-based adhesive (two component unit).

Sika CarboDur plates are non-corroding and have a very high strength which guarantee an excellent durability and fatigue resistance of the system.

The plates have a low regular thickness (1,2mm) and smooth edges without exposed fibres as result of production by pultrusion. Hence, several layers and plate intersections and crossings are simply to execute. The lightweight of the plates enables an easy transportation in rolls and installation (no temporary support needed).

For more information about installation, see document: Recommendations for design and construction of hybrid members (deliverable 5.2).

Figure 4-1: Sika CarboDur

Figure 4-2: Sikadur 30

5   Angles with CFRP-strips

Hybrid angle members considered here are composed of equal leg steel angles, with FRP plates attached to their legs. The investigations carried out during the ANGELHY project refer to applications where these measures are taken in members of lattice tower, either legs or bracings, in order to increase their carrying capacity. The main advantage of such solutions for telecommunication or transmission towers is that the towers are strengthened, without increasing the wind attack areas of the members and therefore without increasing wind or ice loads. In addition, all other advantages of angle section applications in lattice towers, such as good connectivity, good handling or easy transport are still applicable.

The cases examined here refer to attachment of either two CFRP plates on the exterior sides of the legs or of four FRP plates on the exterior and the interior side of the legs, Figure 5-1. The width and length of the FRP plates shall be no larger than the corresponding width/length of the angle legs.

The technological procedures for carrying out the strengthening measures are described in the document: Recommendations for design and construction of hybrid members (deliverable 5.2).
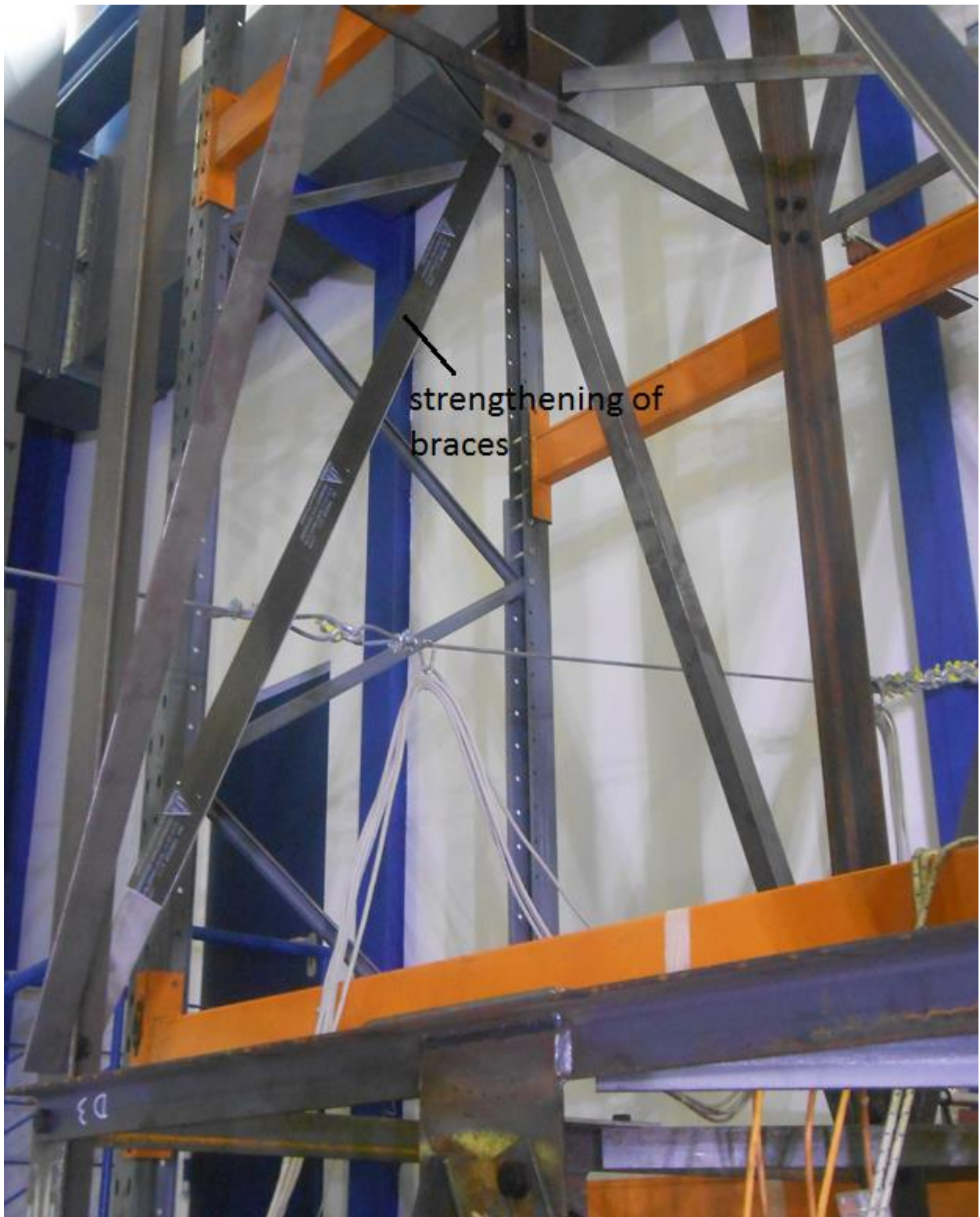

strengthening of legs

Figure 5-1: Strengthening of tower legs and bracing members by CFRP plates

6 Steel lattice towers

6.1 Transmission towers

Lattice towers are used for all ranges of voltages and they are the most common towers types for high-voltage transmission lines. Lattice towers are mainly made of hot-dip galvanized steel angle profiles which are assembled to form a framework (Figure 6-1). The standard height varies from 30m to 60m. In the last years, even height exceeding 100m were achieved with steel lattice towers made of hot-rolled steel angle profiles.
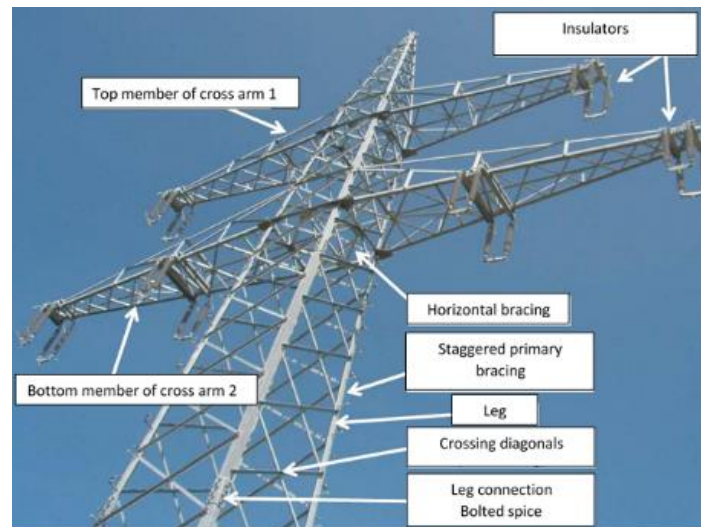

Figure 6-1: Typical typology of a steel lattice transmission tower

The steel angel profiles are applied as single angle members and/or built-up angles. Hereby the star battened connection is the most commonly used for the leg members whereas the back-to-back configuration is mainly used for the primary diagonals.

The primary bracing system is often composed of single unequal angle sections like L60x6, the secondary bracing members are generally made of small single angle sections like L45x4.

The leg members of steel lattice towers mainly bear the self-weight of the tower and are composed of big single equal leg profiles or, in case the load bearing resistance of single angle profiles is insufficient, of closely built-up sections.

The erection of the tower is made on the construction side. First the different modules are preassembled in lying position, then lifted with a crane and finally bolted by assembly operators. Alternatively, the whole tower can be mounted in lying position and then be raised by cable pull. This operation requires a big assembling area and it is therefore only rarely applied. In mountains area, the different modules are often place by helicopter since the mounting area is too confined for cranes.

6.2 Telecommunication towers

Lattice telecom towers are free standing towers composed of three or four legs and a bracing pattern of their vertical or inclined walls. They resist their own self-weight, the self-weight of the antennas and cables they carry, imposed loads and meteorological loads, especially wind loading.

The tower types are all based on a reinforced concrete foundation and they bear antennas, microwave mirrors, antenna and microwave mirror links, waveguides and the vertical ladder for waveguides. The tower members are entirely hot-dip-galvanized and for this purpose welding must be avoided and all connections must be done by hot-dip-galvanized screws. Welding is allowed only for the construction of the towers' footings, the sections of the climbing stair and the lightning arrester of the towers.

Lattice towers are specifically provided for heights ranging from 20m to 80m. Towers are rated heavy or light, according to their design load. Lattice telecom towers have one advantage over pole type towers. The weight of the lattice tower is distributed over a greater area, which reduces the loads on

the foundation and on the ground. The modules of the lattice telecom tower can be assembled one piece at a time and so do not require the use of heavy cranes. A lattice tower can be easily installed even on rough terrain.

Figure 6-2: Steel lattice telecommunication tower

The dimensions of the towers base with square plan is between 1,50m x 1,50m and 12,5m x 12,5m and the foundation of the structure is a concrete slab C20/25 connecting the legs of the tower. The bottom level of the foundation block is between 1,8m and 2,50m below the ground level.

At certain distances along the height, diaphragms are provided that act as platform decks. They consist of UPN or angle sections, forming a rectangular shape which inscribes a rotated square shape, also made of angle sections. The dimensions range from 1,50m x 1,50m to 12,5m x 12,5m.

Triangular lattice towers have dimensions at the base between 2,57m x 2,57m x 2,57m and 6,4m x 6,4m x 6,4m and the bottom level of the foundation block is 2m below the ground level. The legs are made of 60 degrees hot rolled angle profiles and the bracings are made of typical hot rolled angles.

The cross sections of the structural system contain:

• Angle legs from L80x8 to L200x20

• Angle vertical diagonal-bracings from L70x7 to L110x10

• Angle secondary bracings from L25x5 to L55x5

• Horizontals from UPN 80 to UPN 100

• Horizontal diagonals from UPN and angle sections

All towers have:

• Vertical access stair, safety ring and devices against back fall

• Resting platforms are placed at certain distances along the height

• Vertical holsters for feeders, electrical cables, night beacon and lightening system

• There are at least 4 triple band antennas symmetrically placed, typically installed at the upper part and parabolic antennas installed at various heights with diameters ranging from 0,3m to 3,2m.

6.3   Reinforcement measures

The increasing amount of electric current produced by renewable energies require high-voltage transmission lines for its transport. One possibility to comply with the increasing energy demand is the upgrading of existing transmission lines to higher voltage (e.g. from 380-kV to 400-kV).

The increasing demand in telecommunication technologies and the upgrade to G5 requires a high number of new antennas. In addition to the erection of new towers to carry the antennas, antennas will also be added to existing towers.

The above-mentioned developments require the strengthening of the existing tower structures. For transmission and telecommunication towers, the most common strengthening method used in practice is the connection of an additional angle profiles to the leg members (Figure 6-3), the replacement of diagonals with larger angles sections or the adding of additional bracing members.
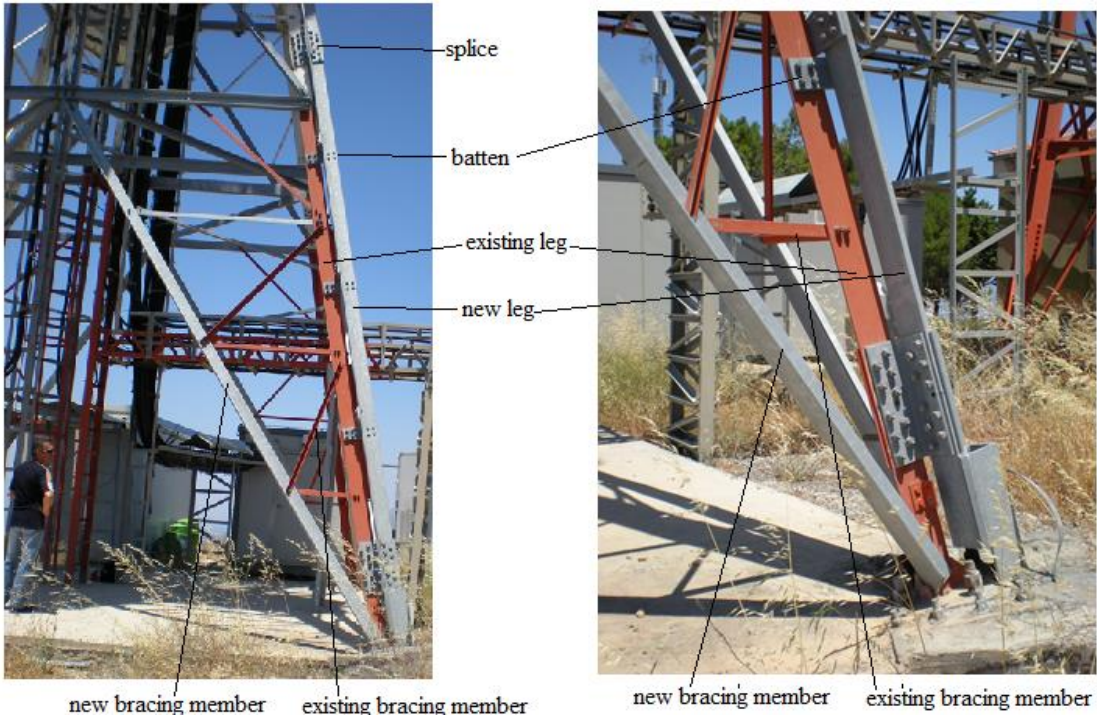
Figure 6-3: Strengthening of existing tower

A new and innovative method to strengthen steel lattice towers is the use of FRP-strips (Figure 6-4). The FRP-plates are applied with an epoxy resin to the sandblasted surface of the angle profiles. This allows a strengthening of the tower without increasing the weight of the structure or its wind and ice attack surface (see also chapter 4 and chapter 5).
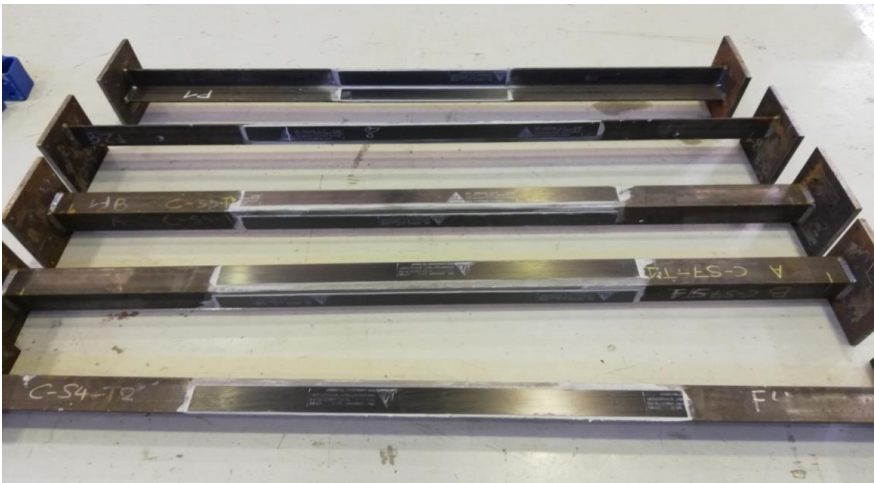
Figure 6-4: Strengthened angle profiles with FRP-strips

The present design guide gives design rules and recommendations for equal leg angles profiles strengthened with FRP plates in chapter 9.

7 Design rules for single angle members

7.1 Cross-section properties

7.1.1 Plastic modulus about strong axis

The plastic modulus about u-u axis can be evaluated equal to $1{,}5 \cdot W_{el,u}$.

For the angle cross-section, due to its lack of symmetry, the $W_{el,u}$ is different for a top fibre (at the tip) or a bottom fibre (at the toe). However, for the design of the cross-section, the most distant fibre from centroid is considered when calculating the elastic modulus (i.e at the tip of the leg), which results in higher stress calculations. In this case, the elastic modulus about u axis can be derived from the following formula:

$$W_{el,u} = \frac{I_u}{0{,}5h\sqrt{2}} \tag{7.1}$$

7.1.2 Plastic modulus about weak axis

The plastic modulus about v axis can be estimated through the following equation by assuming that the radius at the toe of the cross-sections is equal to zero (r=0). The notation of the following formulas is supplemented by Figure 7-1.

$$W_{pl,v} = \frac{A}{2} \cdot (c + d) \tag{7.2}$$

where,

c is the distance between the centre of gravity of the sub-cross-section 2 and the plastic neutral axis (pna), and it can be calculated by the equation:

$$c = \sqrt{2} \cdot \left(\frac{h_2}{2} - y_{G_2}\right) \tag{7.3}$$

d is the distance between the centre of gravity of the sub-cross-section 1 and the pna, and it can be calculated by the equation:

$$d = \sqrt{2} \cdot \left(y_{G_1} - \frac{h_2}{2}\right) \tag{7.4}$$

h_2 is the width of the sub-cross-section 2 and is equal to $h_2 = h - h_1$ $\qquad$ (7.5)

h_1 is the width of the sub-cross-section 1 and is equal to $h_1 = A/4t$ $\qquad$ (7.6)

y_{G_1} is the distance between the centre of gravity of the sub-cross-section 1 and the point O(0,0) along y' axis and it can be calculated by the equation:

$$y_{G_1} = \frac{h_1}{4} + \frac{h_2}{2} + \frac{t}{4} \tag{7.7}$$

y_{G_2} is the distance between the centre of gravity of the sub-cross-section 2 and the point O(0,0) along y' axis and it can be calculated by the equation:

$$y_{G_2} = \frac{h_2^2 + h_2 t - t^2}{4h_2 - 2t} \tag{7.8}$$
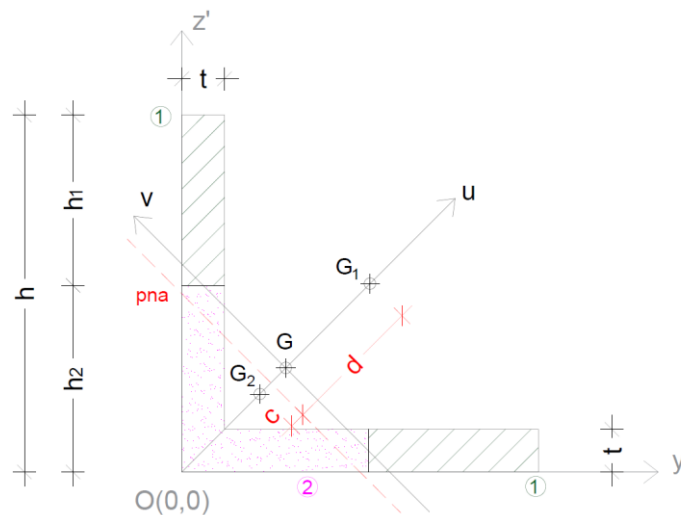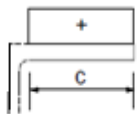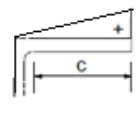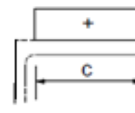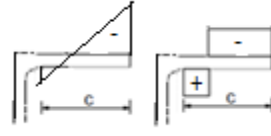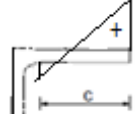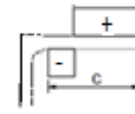
Figure 7-1: Notation for the calculation of the plastic modulus about v axis

7.2 Classification of cross-sections

Equal leg angle cross-sections should be classified by using Table 7-1 below.

Table 7-1: Classification system for equal leg angle cross-sections

	Comment	Class 3	Class 2
Compression N_c		$\frac{c}{t} \leq 13,9\varepsilon$	
Strong axis bending M_u		$\frac{c}{t} \leq 26,3\varepsilon$	$\frac{c}{t} \leq 16\varepsilon$
Weak axis bending M_v	**Tip in tension**	$\frac{c}{t} \leq 30\varepsilon$	
	Tip in compression	$\frac{c}{t} \leq 26,9\varepsilon$	$\frac{c}{t} \leq 14\varepsilon$
ε		$\varepsilon = \sqrt{\frac{235}{f_y}} \; f_y \; in \; \left[\frac{N}{mm^2}\right]$	

7.3 Safety factors

For the steel sections partial safety factors γ_{Mo}, γ_{M1}, γ_{M2} as provided by EN 1993-1-1 [2] apply.

7.4 Resistance of cross-sections

7.4.1 Tension

The design characteristic resistance for cross-sections subjected to tension is equal to:

$$N_{t,Rk} = \frac{Af_y}{\gamma_{M0}}$$
(7.9)

7.4.2 Compression

The design characteristic resistance for class 1, 2 and 3 cross-sections under pure compression is equal to:

$$N_{c,Rk} = \frac{Af_y}{\gamma_{M0}}$$
(7.10)

The design characteristic resistance for class 4 cross-sections under pure compression is equal to:

$$N_{c,Rk} = \frac{A_{eff}f_y}{\gamma_{M0}}$$
(7.11)

where,

A_{eff} is the area of the effective cross-section that equals:

$$A_{eff} = A - 2ct(1 - \rho)$$
(7.12)

where,

ρ is the reduction factor for plate buckling, calculating as follows:

$$\rho = 1 \qquad\qquad \text{for } \bar{\lambda}_p \leq 0{,}748$$
(7.13)

$$\rho = \frac{\bar{\lambda}_p - 0{,}188}{\bar{\lambda}_p^2} \qquad\qquad \text{for } \bar{\lambda}_p > 0{,}748$$
(7.14)

$\bar{\lambda}_p$ is the relative plate slenderness of legs:

$$\bar{\lambda}_p = \sqrt{\frac{\sigma_{com}}{\sigma_{cr}}} = \frac{\frac{c}{t}}{18{,}6\varepsilon}$$
(7.15)

7.4.3 Strong axis Bending

The design characteristic resistance of angle cross-sections subjected to strong axis bending is given by:

$$M_{u,Rk} = W_u \frac{f_y}{\gamma_{M0}}$$
(7.16)

where,

W_u is the parameter modulus about u axis that equals:

$$W_u = \alpha_{i,u}W_{el,u} , \quad i = 2, 3, 4$$
(7.17)

where,

$$\alpha_{2,u} = 1{,}5 \qquad\qquad\qquad \text{for class 1 or 2}$$
(7.18)

$$\alpha_{3,u} = \left[1 + \left(\frac{26{,}3\varepsilon - \frac{c}{t}}{26{,}3\varepsilon - 16\varepsilon}\right) \cdot (1{,}5 - 1)\right] \quad \text{for class 3}$$
(7.19)

$$\alpha_{4,u} = W_{eff,u}/W_{el,u} = \rho_u{}^2 \qquad\qquad \text{for class 4}$$
(7.20)

ρ_u is the reduction factor for plate buckling, calculating as follows:

$$\rho_u = 1 \qquad\qquad \text{for } \bar{\lambda}_p \leq 0{,}748$$
(7.21)

$$\rho_u = \frac{\bar{\lambda}_p - 0{,}188}{\bar{\lambda}_p^2} \qquad\qquad \text{for } \bar{\lambda}_p > 0{,}748$$
(7.22)

$\bar{\lambda}_p$ is the relative plate slenderness of legs:

$$\bar{\lambda}_p = \sqrt{\frac{\sigma_{com}}{\sigma_{cr}}} = \frac{\frac{c}{t}}{35{,}58\varepsilon} \tag{7.23}$$

7.4.4 Weak axis bending

The design characteristic resistance of angle cross-sections to weak axis bending M_v – tip in compression – is given by:

$$M_{v,Rk} = W_v \frac{f_y}{\gamma_{M0}} \tag{7.24}$$

where,

W_v is the parameter modulus about v axis that equals:

$$W_v = \alpha_{i,v} W_{el,v}, \quad i = 2, 3, 4 \tag{7.25}$$

where,

$$\alpha_{2,v} = W_{pl,v}/W_{el,v} \qquad\qquad \text{for class 1 or 2} \tag{7.26}$$

$$\alpha_{3,v} = \left[1 + \left(\frac{26{,}9\varepsilon - \frac{c}{t}}{26{,}9\varepsilon - 14\varepsilon}\right)\cdot\left(\alpha_{2,v} - 1\right)\right] \qquad \text{for class 3} \tag{7.27}$$

$$\alpha_{4,v} = W_{eff,v}/W_{el,v} = 0{,}94\cdot\rho_v^2 \qquad\qquad \text{for class 4} \tag{7.28}$$

ρ_v is the reduction factor for plate buckling, calculating as follows:

$$\rho_v = 1 \qquad\qquad \text{for } \bar{\lambda}_p \leq 0{,}748 \tag{7.29}$$

$$\rho_v = \frac{\bar{\lambda}_p - 0{,}188}{\bar{\lambda}_p^2} \qquad\qquad \text{for } \bar{\lambda}_p > 0{,}748 \tag{7.30}$$

$\bar{\lambda}_p$ is the relative plate slenderness of legs:

$$\bar{\lambda}_p = \sqrt{\frac{\sigma_{com}}{\sigma_{cr}}} = \frac{\frac{c}{t}}{36{,}48\varepsilon} \tag{7.31}$$

The design characteristic resistance of angle cross-sections to weak axis bending M_v – tip in tension – is given by:

$$M_{v,Rk} = W_{pl,v} \frac{f_y}{\gamma_{M0}} \tag{7.32}$$

where,

$W_{pl,v}$ is the plastic modulus about v axis; eq. (7.2) – (7.8) may be used for the calculation.

7.5 Buckling resistance of members

7.5.1 Buckling resistance in compression

The design buckling resistance of a compression member should be taken as:

$$N_{b,Rd} = \frac{\chi_{min} A f_y}{\gamma_{M1}} \qquad\qquad \text{for Class 1,2 and 3 cross-sections} \tag{7.33}$$

$$N_{b,Rd} = \frac{\chi_{min} A_{eff} f_y}{\gamma_{M1}} \qquad\qquad \text{for Class 4 cross-sections} \tag{7.34}$$

where,

χ_{min} is the buckling reduction factor which should be determined as a function of the relative slenderness $\bar{\lambda}$ of the compression member;

A_{eff} is the area of the effective cross-section calculated by the equations (7.12)-(7.15), using the following value for the relative plate slenderness of legs:

$$\bar{\lambda}_p = \sqrt{\chi_{min}} \frac{\frac{c}{t}}{18,6\varepsilon} \tag{7.35}$$

The buckling reduction factor should be determined as a function of the relative slenderness $\bar{\lambda}$ of the compression member for the flexural buckling modes only:

$$\chi_{min} = \{\chi_u; \chi_v\} \tag{7.36}$$

The relative slenderness $\bar{\lambda}$ should be taken as:

$$\bar{\lambda} = \sqrt{\frac{Af_y}{N_{cr}}} \tag{7.37}$$

where,

N_{cr} is the minimum elastic critical force for the flexural buckling mode based on the gross cross-sectional properties, i.e $N_{cr}=\min\{N_{cr,u};N_{cr,v}\}$

$N_{cr,u}$ for elastic flexural buckling about u-u, leading to $\overline{\lambda_u}$;

$N_{cr,v}$ for elastic flexural buckling about v-v, leading to $\overline{\lambda_v}$;

The value of the buckling reduction factor χ for the appropriate relative slenderness $\bar{\lambda}$ should be determined from the relevant buckling curve according to the equations (8.73)-(8.74) in combination with tables 8.2 and 8.3 of prEN 1993-1-1: §8.3.1.3 [1], i.e curve b is used for steel grades S235-S420 while curve a is used for steel higher grades (≥S460).

7.5.2 Buckling resistance for strong axis bending

The design buckling resistance moment of a laterally unrestrained beam should be taken as:

$$M_{u,Rd} = \chi_{LT} W_u \frac{f_y}{\gamma_{M1}} \tag{7.38}$$

where,

χ_{LT} is the buckling reduction factor which should be determined as a function of the relative slenderness $\overline{\lambda_{LT}}$ of the compression member;

W_u is the parameter modulus about u axis calculated by the equations (7.17)-(7.23), using the following value for the relative plate slenderness of legs:

$$\bar{\lambda}_p = \sqrt{\chi_{LT}} \frac{\frac{c}{t}}{35,58\varepsilon} \tag{7.39}$$

The reduction factor for lateral torsional buckling χ_{LT} should be determined as a function of the relative slenderness $\overline{\lambda_{LT}}$ of the member:

$$\overline{\lambda_{LT}} = \sqrt{\frac{W_u f_y}{M_{cr}}} \tag{7.40}$$

where,

W_u is the parameter modulus about u axis, see equations (7.17)-(7.23);

The elastic critical moment for lateral-torsional buckling is given by the following equation, with use of Table 7-2:

$$M_{cr} = C_b \frac{0,46 \cdot E \cdot h^2 \cdot t^2}{l} \tag{7.41}$$

Table 7-2: Determination of the C_b-factor for LTB

<u>**General case:**</u>

$$C_b = \frac{12,5 M_{max}}{2,5 M_{max} + 3 M_A + 4 M_B + 3 M_C} \leq 1,5$$

<u>**For linear moment distribution:**</u>

$$C_b = \frac{12,5}{7,5 + 5\psi} \quad \text{with} \quad -1 \leq \psi = \frac{M_2}{M_1} \leq 1$$

The value of the buckling reduction factor χ_{LT} for the relative slenderness $\overline{\lambda_{LT}}$ should be derived from buckling curve **a**. The buckling curve can be determined by the equation (6.57) of EN 1993-1-1: §6.3.2.3(1) [2] for lateral-torsional buckling, using $\bar{\lambda}_{LT,0} = 0,4$ and β=1,00 (see equations below).

$$\chi_{LT} = \frac{1}{\Phi_{LT} + \sqrt{\Phi_{LT}^2 - \bar{\lambda}_{LT}^2}} \quad \text{but} \quad \begin{cases} \chi_{LT} \leq 1,0 \\ \chi_{LT} \leq 1/\bar{\lambda}_{LT}^2 \end{cases} \tag{7.42}$$

$$\Phi_{LT} = 0,5 \left[1 + a_{LT} \left(\bar{\lambda}_{LT} - 0,4 \right) + \bar{\lambda}_{LT}^2 \right] \tag{7.43}$$

Lateral torsional buckling may be ignored and χ_{LT} set equal to 1,0 when one of the following conditions apply:

- $\bar{\lambda}_{LT} \leq \bar{\lambda}_{LT,0}$ with $\bar{\lambda}_{LT,0} = 0,4$

- $\frac{M_{Ed}}{M_{cr}} \leq \bar{\lambda}_{LT,0}^2$

- $\frac{N_{Ed}}{N_{bu,Rd}} > 0,5$

- $\frac{N_{Ed}}{N_{bv,Rd}} > 0,5$

7.5.3 Buckling resistance for weak axis bending

The design resistance of angle cross-sections to weak axis bending M_v – tip in compression – is:

$$M_{v,Rd} = M_{v,Rk} \tag{7.44}$$

The design resistance of angle cross-sections to weak axis bending M_v – tip in tension – is:

$$M_{v,Rd} = M_{v,Rk} \tag{7.45}$$

7.5.4 Resistance to combined compression and bending

For angle members subjected to compression and bending, two checks for buckling around one or the other principal axis should be satisfied.

- <u>strong axis check</u>

$$\left(\frac{N_{Ed}}{N_{bu,Rd}} + k_{uu} \frac{M_{u,Ed}}{M_{u,Rd}} \right)^\xi + k_{uv} \frac{M_{v,Ed}}{M_{v,Rd}} \leq 1 \tag{7.46}$$

- <u>weak axis check</u>

$$\left(\frac{N_{Ed}}{N_{bv,Rd}} + k_{vu} \frac{M_{u,Ed}}{M_{u,Rd}} \right)^\xi + k_{vv} \frac{M_{v,Ed}}{M_{v,Rd}} \leq 1 \tag{7.47}$$

where,

k_{ij} are the interaction factors that are provided in Table 7-3;

ξ is a factor that depends on the cross-section class.

<div align="center">**Table 7-3: Determination of k_{ij} factors**</div>

<div align="center">k_{ij} factors</div>

$$k_{uu} = \frac{C_u}{1-\frac{N_{Ed}}{N_{cr,u}}} \qquad\qquad k_{uv} = C_v$$

$$k_{vu} = C_u \qquad\qquad k_{vv} = \frac{C_v}{1-\frac{N_{Ed}}{N_{cr,v}}}$$

$$C_u = 0,6+0,4\psi_u \qquad\qquad C_v = 0,6+0,4\psi_v$$

$$-1 \le \psi_u = \frac{M_{2u}}{M_{1u}} \le 1 \qquad\qquad -1 \le \psi_v = \frac{M_{2v}}{M_{1v}} \le 1$$

The ξ-factor is:

$$c/t \le 16\varepsilon: \qquad\qquad \xi = 2 \tag{7.48}$$

$$16\varepsilon < c/t < 26,3\varepsilon: \qquad \xi = \left[1 + \left(\frac{26,3\varepsilon - \frac{c}{t}}{26,3\varepsilon - 16\varepsilon}\right) \cdot (2-1)\right] \tag{7.49}$$

$$c/t > 26,3\varepsilon: \qquad\qquad \xi = 1 \tag{7.50}$$

7.5.5 The general method for equal leg angles

The general method applies to lateral and lateral torsional buckling for structural components with mono symmetric cross-sections, built-up or not, uniform or not, with complex support conditions or not, which are subject to compression and/or bi-axial bending in the plane, but which do not contain rotated plastic hinges. In this section, the general method is specified and presented for equal leg angle members, after it has been adjusted appropriately.

The out-of-plane buckling resistance of the member is sufficient if the following equation satisfies:

$$\chi_{op} \cdot \frac{a_{ult,k}}{\gamma_{M1}} \ge 1,0 \tag{7.51}$$

where,

χ_{op} is the reduction factor corresponding to the non-dimensional slenderness $\overline{\lambda_{op}}$ and aimed at accounting for weak axis buckling only, as it has been shown from previous sections to be the predominate failure mode. Therefore, $\chi_{op} = \min\{\chi_u; \chi_v\}$. The selection of the buckling curve is based on [2].

$a_{ult,k}$ is the minimum load amplifier of the design loads to reach the characteristic resistance of the most critical cross-section of the structural component considering its in plane behaviour without taking lateral or lateral torsional buckling into account, but however accounting for all effects due to in plane geometrical deformation and imperfections, global and local, where relevant. It can be derived from the following equation:

$$\frac{1}{\alpha_{ult,k}} = \frac{\sigma_{max}}{f_y} = \frac{\sigma_N}{f_y} + \frac{\sigma_{e_0}}{f_y} + \frac{\sigma_M}{f_y} \tag{7.52}$$

in which:

- the first term relates to the stress under pure compression;

- the second, to the second order maximum stress resulting from the amplification of the first order moment $N_{Ed} \cdot e_{0,EC3}$ ($e_{0,EC3}$ is the equivalent imperfection as defined in[2]), i.e. the moment $N_{Ed} \cdot e_{0,EC3}[1/(1-N_{Ed}/N_{cr,u})]$;

- the third one relates to the second order maximum stress resulting from the amplification of the first order moment $N_{Ed} \cdot e_v$ (e_v is the load eccentricity), which can be estimated as $N_{Ed} \cdot e_v[1/(1-N_{Ed}/N_{cr,u})]$.

The global relative slenderness $\overline{\lambda_{op}}$ for the structural component should be determined from the equation below, in which the term $\alpha_{cr,op}$ is the minimum load amplifier for the design loads to reach the elastic critical load of the structural component associated to weak axis buckling.

$$\overline{\lambda_{op}} = \sqrt{\frac{\alpha_{ult,k}}{\alpha_{cr,op}}} \qquad (7.53)$$

In case that the angle is connected by the leg, the "in-plane" instability effects may be considered as negligible, 2nd order effects may be disregarded ($1/(1-N_{Ed}/N_{cr,u})=1$) and e_0 may be taken equal to zero (in recognition of the rather limited impact of this parameter);

The cross-section resistance in bending may be evaluated by using eq. (7.17)-(7.23). On the safe side, the elastic cross-section resistance (W_{el}) may be used.

8   The "leg-segment instability" mode

A "segment instability" is defined as an instability mode associated to the buckling of more than one member forming a segment. In the present case the instability is associated to the buckling of the two diagonals of a leg of a transmission tower (see Figure 8-1) and therefore will be named as "leg-segment instability". The diagonals move laterally and bends about an axis parallel to one of their angle legs while the exterior leg rotates about its longitudinal axis. The elements which "close the horizontal leg triangles" do not undergo any deformation; they are just translated.

The leg consists of three vertically oriented members: the main or "exterior" leg and the two diagonals (1 & 2) that are connected with a number of horizontal bars and bracing members forming "triangles".

Each of the two diagonals and the main leg member (exterior one) constituting the segment should be individually stable and should be able to resist to the applied maximum forces, as they have been initially designed to that.
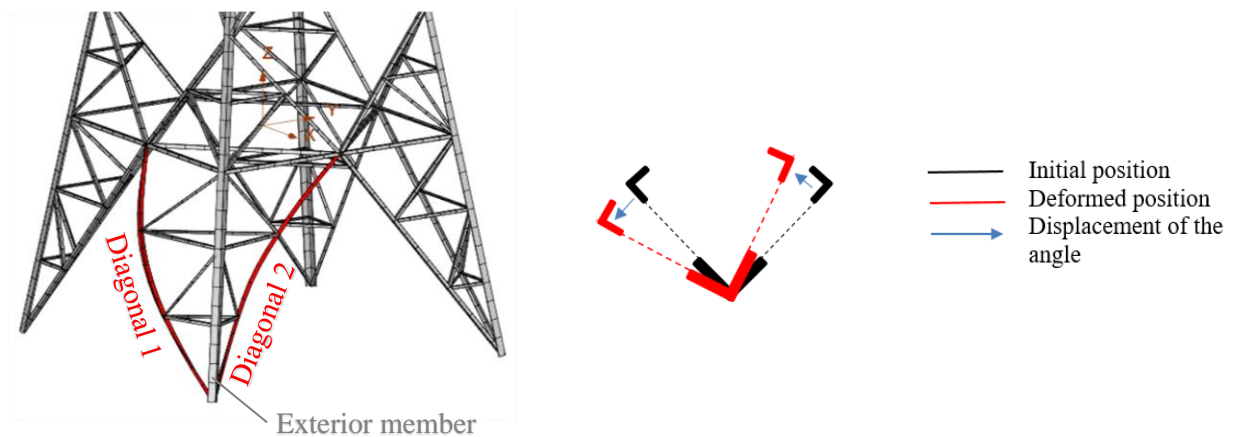
Figure 8-1: Elastic instability mode of the segment (left) and deformation of the members through a horizontal cut in the leg (right)

8.1 Proposed models for the segment instability

8.1.1   Simplified model

The equivalent model is illustrated in Figure 8-2. The two parallel vertical members represent the two diagonals and the horizontal pinned members, the elements "closing the triangle". Both diagonals are assumed to be made of the same profile, as it happens mostly in practise. The extremities of the vertical members are assumed to be pinned; this is what is expected at the foundation level, while at the top, the very small restraining effect resulting from the actual continuity of the diagonals is neglected.

The deformed shape of the system is seen on the right sketch (Figure 8-2).
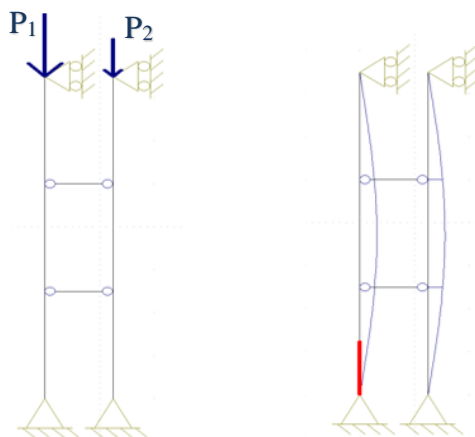
Figure 8-2: Equivalent model of the leg (left) and deformed shape (right)

For this simplified model, the critical load multiplier a_{cr} may be given by the following formula:

$$a_{cr} = \frac{2\pi^2 EI_y}{L^2.(P_1+P_2)} \qquad (8.1)$$

where,

 I_y is the moment of inertia about y-y geometrical axis (see Figure 2-1) of the diagonal's cross-section;

 L   is the buckling length of the diagonal;

 E   is the modulus of elasticity;

 P_1, P_2 are the axial forces in the two diagonals.

This model is independent of the number of horizontal "rigid triangles", and therefore may be generally used for segments with pyramidal configuration.

8.1.2 Final model

In this final model illustrated in Figure 8-3, the beneficial effect of the torsional stiffness is taken into account, and it is considered that the axial force in the exterior member is not influencing its torsional stiffness.
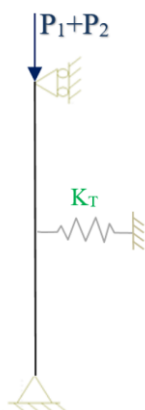
Figure 8-3: Final proposed design model

For the final model, the critical load multiplier a_{cr} is equal to:

$$a_{cr} = \frac{N_{cr}}{P_1+P_2} \qquad (8.2)$$

where,

 N_{cr} is the critical load of the equivalent column representing the segment;

 P_1, P_2 are the axial applied forces in the two diagonals.

The critical load of the equivalent column can be evaluated by Eq.(8.3):

$$N_{cr} = \frac{\pi^2 E I_{y,tot}}{L^2} + \frac{3}{16} K_T L \tag{8.3}$$

where,

$I_{y,tot}$ is the total moment of inertia about y-y geometrical axis of both diagonals (i.e $I_{y,tot}=2I_y$);

L   is the buckling length of the diagonal;

E   is the modulus of elasticity;

K_T is the stiffness of the unique spring restraint, equals $\frac{4}{m^2}(2R_{mean})$.

m   is the number of zones of length of the leg ($l = L/m$ separated by rigid horizontal triangles in the leg); the accuracy of the formulae for K_T is sufficient for a value of m≤6 (i.e for maximum 5 horizontal rigid triangles in the leg).

The mean value of the lateral restraint R of the diagonals is calculated as follows:

$$R_{mean} = \frac{3C}{2L_{ext}} \cdot \frac{1}{n} \sum_{i=1}^{n} \frac{1}{d_i^2} \tag{8.4}$$

where:

C   is the torsional rigidity of the cross-section and is approximately equal to:

$$C = \frac{G}{3} \sum hb^3 = \frac{G}{3} \cdot 2 \cdot (h - 0{,}5t)t^3 \tag{8.5}$$

L_{ext} is the length of the exterior (main) member of the leg;

d_i is the horizontal distance of the longitudinal axis of the diagonal from the longitudinal axis of the main leg, where i is the index for the horizontal level (see Figure 8-4).
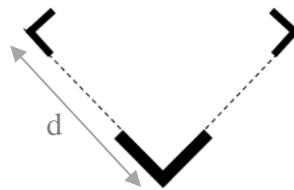
Figure 8-4: Determination of distance d

8.2 Ultimate resistance of the leg

For both proposed models, an estimation of the carrying capacity of the column in compression can be done by the Merchant-Rankine approach:

$$\frac{1}{a_u} = \frac{1}{a_{cr}} + \frac{0{,}96}{a_{pl}} \tag{8.6}$$

where α_{cr} can be estimated with one of the above-mentioned proposed models, and α_{pl} can be evaluated by the following equation:

$$\alpha_{pl} = \frac{2 \cdot N_{pl}}{P_1 + P_2} \tag{8.7}$$

where:

N_{pl} is the plastic resistance of the diagonal's cross-section ($N_{pl}=Af_y$)

9 Design rules for hybrid angle members

9.1 Cross-section properties

The design rules refer to rolled angle sections with strengthening by CFRP plates placed on the outer side of both legs. The CFRP plates are attached to the tip of the legs, their width being equal or smaller than the width of the angle legs as shown in Figure 9-1. The design rules listed in the following assume full shear connection between steel and CFRP surfaces as observed during the ANGELHY experimental investigations.
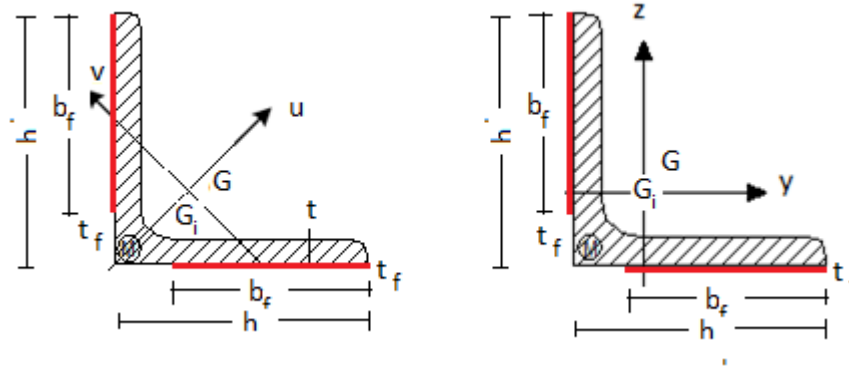
G$_i$ centroid of hybrid section, G centroid of steel section

Figure 9-1: Notation, principal and geometric axes for hybrid section

The hybrid steel-CFRP section will be transformed to an entirely steel section with equivalent cross-section properties, denoted with the subscript i.

Modular ratio between steel and FRP material: $n = \dfrac{E_s}{E_f}$ (9.1)

Cross-section area of equivalent section: $A_i = A + \dfrac{A_f}{n}$ (9.2)

where,

$A_f = 2 \cdot b_f \cdot t_f$ is the cross-section area of the CFRP plates

9.1.1 Principal axes

Position of centroid

$v_{Gi} = 0$ (9.3)

$$u_{Gi} = \frac{A_s \cdot u_{Gs} + \frac{A_f}{n} \cdot u_{Gf}}{A_i}$$ (9.4)

where:

$u_{Gf} = \dfrac{\left(h - \frac{b_f}{2}\right)}{\sqrt{2}}$ is the position of the centroid of the CFRP plates

Second moment of area, weak axis

$$I_{vi} = I_{vs} + A_s \cdot (u_{Gi} - u_{Gs})^2 + \frac{A_f}{n} \cdot \left(u_{Gi} - u_{Gf}\right)^2$$ (9.5)

Second moment of area, strong axis

$$I_{ui} = I_{us} + \frac{h^3 - (h-b)^3}{3 \cdot n} \cdot t$$ (9.6)

9.1.2 Geometric axes

Position of centroid

$$y_{Gi} = z_{Gi} = u_{Gi} \frac{\sqrt{2}}{2} \tag{9.7}$$

Second moment of area

$$I_{yi} = I_{ys} + A_s.(y_{Gi} - y_{Gs})^2 + \frac{A_f}{2n} \cdot y_{Gi}^2 + \frac{A_f}{2n} \cdot \left(z_{Gi} - \left(h - \frac{b_f}{2}\right)\right)^2 \tag{9.8}$$

$$I_{zi} = I_{yi} \tag{9.9}$$

9.2 Classification of cross sections

The steel cross-sections studied throughout the ANGELHY project, were rolled angle sections of class 2 or class 3 according to Table 7-1.

Therefore, the section classification according of hybrid cross-sections is done according to Table 7-1.

It is expected that the presence of CFRP plates lead to a reduction of the cross-section class. However, this is not implied here since such sections were not studied during ANGELHY.

9.3 Safety factors

Safety factors are to be used depending on the regulations used in the specific design. Such regulations exist in the form of design guidelines in Europe. They are listed in the followings.

- Technical Report n°55, Third Edition (2012): Design guidance for strengthening concrete structures using fibre composite materials, based on Eurocode 2, part 1-1 (England).

- AFGC 2011: Réparation et Renforcement des Structures en béton au moyen des Matériaux Composites, based on Eurocode 2, part 1-1 (France).

- CNR-DT 200 R1/2013: Istruzioni per la Progettazione, l'Esecuzione ed il Controllo di Interventi di Consolidamento Statico mediante l'utilizzo di Compositi Fibrorinforzati (Italy).

- Fib 14 (2001) : Design and use of externally bonded fibre reinforced polymer reinforcement (FRP EBR) for reinforced concrete structures, based on Eurocode 2, part 1-1 (Switzerland).

For the steel sections partial safety factors γ_{Mo}, γ_{M1}, γ_{M2} as provided by [2] apply.

The partial safety factor for CFRP plates is denoted as γ_f.

For CFRP material as additional conversion factor, denoted as η, is applied.

9.4 Resistance of cross-sections

9.4.1 Tension

$$N_{t,Rd} = A_s \cdot \frac{f_y}{\gamma_{M0}} + A_f \cdot \frac{\eta \cdot f_f}{\gamma_f} \tag{9.10}$$

9.4.2 Compression

$$N_{c,Rd} = A_s \cdot \frac{f_y}{\gamma_{M1}} + A_f \cdot \frac{\eta \cdot k \cdot f_f}{\gamma_f} \qquad (9.11)$$

The reduction factor of the FRP strength for pure compression is k = 0,5.

9.4.3 Bending

Design moment resistance to strong axis bending

$$M_{u,Rd} = M_{u,pl,s,Rd} + \frac{\eta \cdot f_f \cdot t_f \cdot b \cdot (2b-h)}{3\sqrt{2} \cdot \gamma_f} \qquad (9.12)$$

where $M_{u,pl,s,Rd}$ is the design moment resistance of the steel section for strong axis bending

Design moment resistance to weak axis bending

$$M_{v,Rd} = \frac{f_y \cdot t}{\sqrt{2} \cdot \gamma_{M0}} \cdot \{(h-x_0)^2 + x_0^2\} + \frac{2 \cdot \eta \cdot f_f \cdot t_f}{3 \cdot \sqrt{2} \cdot (h-x_0) \cdot \gamma_f} \left\{ (h-x_0)^3 + \left[x_0 - (h-b_f) \right]^3 \right\} \qquad (9.13)$$

where,

$$x_0 = \frac{\frac{b}{2} - \sqrt{\left(\frac{b}{2}\right)^2 - ac}}{a} \qquad (9.14)$$

$$a = 2f_s t \qquad (9.15)$$

$$b = 3f_s th + f_f t_f b_f \qquad (9.16)$$

$$c = f_s th^2 - f_f t_f b_f \left(\frac{b_f}{2} - h\right) \qquad (9.17)$$

9.4.4 Resistance to combined axial force and bending

Tension axial force

$$\frac{N_{Ed}}{N_{t,Rd}} + \frac{M_{u,Ed}}{M_{u,,Rd}} + \frac{M_{v,Ed}}{M_{v,,Rd}} \le 1.0 \qquad (9.18)$$

Compression axial force

$$\left(\frac{N_{Ed}}{N_{c,Rd}} + \frac{M_{u,Ed}}{M_{u,Rd}}\right)^2 + \frac{M_{v,Ed}}{M_{v,,Rd}} \le 1 \qquad (9.19)$$

9.5 Buckling resistance of members

9.5.1 Buckling resistance in compression

$$N_{b,Rd} = \min\{N_{bu,Rd}, N_{bv,Rd}\} \qquad (9.20)$$

where,

$$N_{bu,Rd} = \chi_u \cdot N_{c,Rd} \qquad (9.21)$$
$$N_{bv,Rd} = \chi_v \cdot N_{c,Rd} \qquad (9.22)$$

Slenderness

$$\bar{\lambda}_u = \sqrt{\frac{N_{c,R}}{N_{cr,u}}} \qquad (9.23)$$

$$\bar{\lambda}_v = \sqrt{\frac{N_{c,R}}{N_{cr,v}}} \qquad (9.24)$$

Critical buckling loads

$$N_{cr,u} = \frac{\pi^2 \cdot E_S \cdot I_{ui}}{l^2} \tag{9.25}$$

$$N_{cr,v} = \frac{\pi^2 \cdot E_S \cdot I_{vi}}{l^2} \tag{9.26}$$

Reduction factors

χ_u, χ_v as functions of the slenderness derived from buckling curve **b**
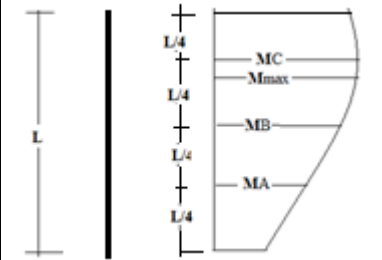
9.5.2 Lateral torsional buckling resistance

$$M_{b,Rd} = \chi_{LT} \cdot M_{u,Rd} \tag{9.27}$$

- **Determination of χ_{LT}**

Critical LTB moment: $M_{cr} = C_b \dfrac{0,46 \cdot E \cdot h^2 \cdot \left(t + \frac{t_f}{n}\right)^2}{l}$ (9.28)

Table 9-1: C_b factor for the determination of the critical LTB moment

$C_b = \dfrac{12.5 M_{\max}}{2.5 M_{\max} + 3 M_A + 4 M_B + 3 M_C} \le 1.5$ For linear moment distribution with -1 $\le\psi=\frac{M_2}{M_1}\le$1 $C_b = \dfrac{12,5}{7,5 + 5\psi}$	

Slenderness to LTB $\bar{\lambda}_{LT} = \sqrt{\dfrac{M_{u,R}}{M_{cr}}}$ (9.29)

Reduction factor χ_{LT} as function of the LTB slenderness derived from buckling curve **d**

Based on [2], lateral torsional buckling effects need not be considered and χ_{LT} is set to $\chi_{LT} = 1$ when one of the following conditions apply:

- $\bar{\lambda}_{LT} \le \bar{\lambda}_{LT,0}$ with $\bar{\lambda}_{LT,0}$=0,4 (9.30)
- $\dfrac{M_{Ed}}{M_{cr}} \le \bar{\lambda}_{LT,0}^2$ (9.31)
- $\dfrac{N_{Ed}}{N_{bu,Rd}} > 0,5$ (9.32)
- $\dfrac{N_{Ed}}{N_{bv,Rd}} > 0,5$ (9.33)

9.5.3 Resistance to combined compression and bending

Strong axis check

$$\left(\frac{N_{Ed}}{N_{bu,Rd}} + k_{uu} \frac{M_{u,Ed}}{M_{b,Rd}}\right)^{\xi} + k_{uv} \frac{M_{v,Ed}}{M_{v,Rd}} \le 1 \tag{9.34}$$

Weak axis check

$$\left(\frac{N_{Ed}}{N_{bv,Rd}} + k_{vu}\frac{M_{u,Ed}}{M_{b,Rd}}\right)^{\xi} + k_{vv}\frac{M_{v,Ed}}{M_{v,Rd}} \leq 1 \tag{9.35}$$

Factors

$$k_{uu} = \frac{C_u}{1-\frac{N_{Ed}}{N_{cr,u}}} \tag{9.36}$$

$$k_{uv} = C_v \tag{9.37}$$

$$k_{vu} = C_u \tag{9.38}$$

$$k_{vv} = \frac{C_v}{1-\frac{N_{Ed}}{N_{cr,v}}} \tag{9.39}$$

$$C_u = 0{,}6+0{,}4\psi_u \quad -1 \leq \psi_u = \frac{M_{2u}}{M_{1u}} \leq 1 \tag{9.40}$$

$$C_v = 0{,}6+0{,}4\psi_v \quad -1 \leq \psi_v = \frac{M_{2v}}{M_{1v}} \leq 1 \tag{9.41}$$

$$\xi = 2 \tag{9.42}$$

10 Design rules for closely spaced built-up angle members

10.1 Cross section of built-up sections

In the present design guideline design rules for two different configurations of closely spaced built-up angles are given: back to back and star battened back to back built-up sections. These rules have been developed for compact sections of class 1 or class 2. Cross sections of class 3 and 4 are outside the scope of the following design proposals.

10.1.1 Back to back built-up sections

The configuration of the back to back built-up sections is shown in Figure 10-1.
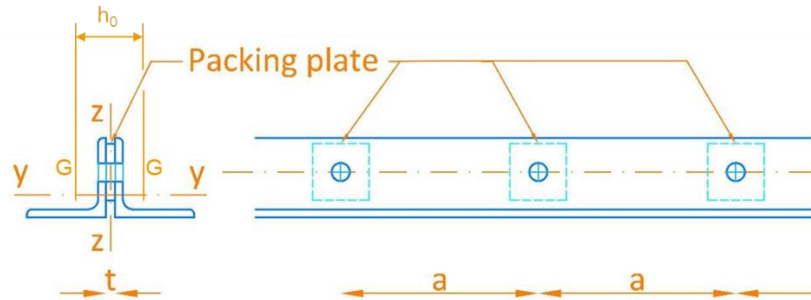
Figure 10-1: Back to back built-up sections

where,

z-z   -   Major axis
y-y   -   Minor axis
h_0 Distance between the centroids
a   Distance between the packing plates
i_v Radius of gyration about the angle section's minor axis (see Figure 2-1)
L   Member length
i_z Radius of gyration of the built-up section member considered as integral about z-z
$A^{'}$ Cross-sectional area of the built-up section

10.1.2 Star battened back to back built-up sections

The configuration of the star battened back to back built-up sections is shown in Figure 10-2.

The built-up section can be composed of angles with equal or unequal size.
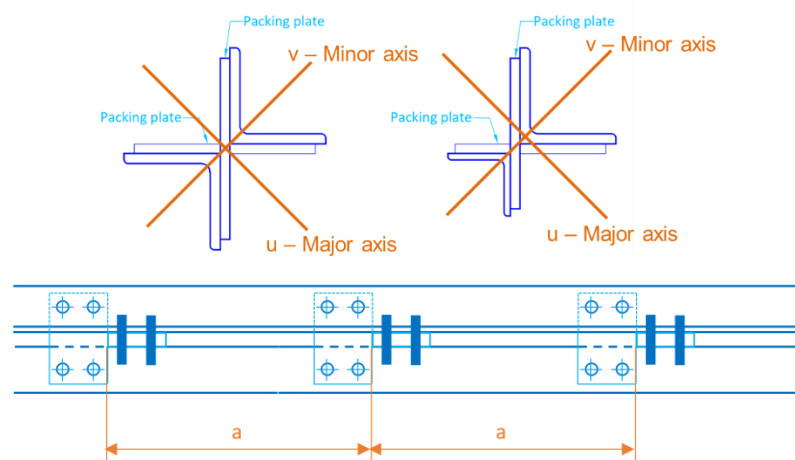

Figure 10-2: Star battened back to back built-up sections

where,

v-v - Major axis

u-u - Minor axis

h_0 Distance between the centroids of the angle sections

a   Distance between the packing plates

i_v Radius of gyration about the angle section's minor axis (see Figure 2-1)

L   Member length

i_z Radius of gyration of the built-up section member considered as integral about z-z

A'   Cross-sectional area of the built-up section

10.2 Safety factors

For the steel sections partial safety factors γ_{M1} and γ_{M2} as provided by [2] apply.

10.3 Buckling resistance of back to back connected built-up sections

10.3.1 General

The following design approach may be applied if at least two intermediate pairs of batten plates are used along the built-up member. Each batten plate should contain at least four bolts as shown in Figure 10-2.

10.3.2 Buckling resistance in compression – flexural buckling about strong axis

The design buckling resistance of a compression member should be taken as:

$$N_{bz,Rd} = \frac{\chi_z A' f_y}{\gamma_{M1}}$$

(10.1)

χ_z: is the buckling reduction factor determined based on the slenderness $\bar{\lambda}_{Sv}$ and buckling curve b

The relative slenderness $\bar{\lambda}_{Sv}$ should be taken as:

$$\bar{\lambda}_{Sv} = \sqrt{\frac{A' f_y}{N_{cr,Sv}}}$$

(10.2)

The critical axial force $N_{cr,SV}$ considering the influence of the shear stiffness is calculated as follows:

$$N_{cr,Sv} = \frac{1}{\frac{1}{N_{cr}} + \frac{1}{S_v}}$$

(10.3)

where,

$\quad$ N_{cr} is the critical axial force of the built-up member considered as integral neglecting the influence of the shear stiffness

$\quad$ S_v is the shear stiffness of the built-up member

S_v is determined in depending of the connection type as follows:

$$S_v = S_{v1} = \frac{1}{\frac{a^2}{24EI_{v,ch}}} \qquad \text{For members connected through fit bolts}$$

(10.4)

$$S_v = S_{v2} = \frac{1}{\frac{a^2}{24EI_{v,ch}} + \frac{ah_0}{12EI_{pp}}} \text{ For members connected preloaded bolts}$$

(10.5)

where,

$\quad$ $I_{v,ch}$ is the 2nd moment of area of one angle section about its minor axis

$\quad$ I_{pp} is the 2nd moment of area of the effective part of the packing plate

$$I_{pp} = \frac{\pi(B+2t+t_p)^4 - \pi d^4}{64} \tag{10.6}$$

where,

t:	is the thickness of the angle section
t_p:	is the thickness of the packing plate
B:	is the inside diameter of the bolt head (noted s in EN 14399 [3])
d:	is the diameter of the hole

S_{v2} may also be applied if the design slip resistance $F_{s,Rd}$ for non-fully preloaded bolt connections is higher than the shear force to be transmitted.

10.3.3 Buckling resistance in compression – flexural buckling about weak axis

The design buckling resistance of a compression member should be taken as:

$$N_{by,Rd} = \frac{\chi_y A' f_y}{\gamma_{M1}} \tag{10.7}$$

χ_y: is the buckling reduction factor determined based on the slenderness $\bar{\lambda}_{y'}$ and buckling curve b

The relative slenderness $\bar{\lambda}_{y'}$ should be taken as:

$$\bar{\lambda}_{y'} = \sqrt{\frac{A' f_y}{N_{cr,y'}}} \tag{10.8}$$

The critical axial force $N_{cr,y'}$ considering the influence of the shear stiffness is calculated as follows:

$$N_{cr,y'} = \frac{\pi^2 E I_{y'}}{L_{cr,y'}^2} \tag{10.9}$$

where,

$I_{y'}$	is the 2nd moment of area of the built-up member around the weak axis
$L_{cr,y'}$:	is the buckling length of the built-up member for buckling around the weak axis

10.3.4 Resistance of the connection

The resistance of the connection should be verified according to EN 1993-1-8 [4] based on the shear force V_{Ed} calculated as follows:

$$V_{Ed} = \frac{\pi}{L} \frac{a}{h_0} M_{Ed} \tag{10.10}$$

$$M_{Ed} = \frac{N_{Ed}\frac{L}{200}}{1 - \frac{N_{Ed}}{N_{cr,Sv}}} \tag{10.11}$$

where,

N_{Ed}	is the axial forces in the built-up sections for the governing load case

10.4 Buckling resistance of star battened built-up sections

10.4.1 Buckling resistance in compression – flexural buckling about strong axis

The design buckling resistance of a compression member should be taken as:

$$N_{bu,Rd} = \frac{\chi_u A' f_y}{\gamma_{M1}} \tag{10.12}$$

The buckling reduction factor χ_u is based on the slenderness $\bar{\lambda}_{u,Sv}$ and buckling curve b

$$\bar{\lambda}_{Sv} = \sqrt{\frac{A' f_y}{N_{cr,u,Sv}}} \tag{10.13}$$

The critical axial force $N_{cr,u,Sv}$ considering the influence of the shear stiffness is calculated as follows:

$$N_{cr,u,Sv} = \frac{1}{\frac{1}{N_{cr,u}} + \frac{1}{S_v}} \tag{10.14}$$

where,

$N_{cr,u}$ is the critical axial force of the built-up member considered as integral neglecting the influence of the shear stiffness

S_v is the shear stiffness of the built-up member

S_v is determined in depending of the connection type as follows:

$$S_v = S_{v1} = \frac{1}{\frac{a^2}{24EI_{v,ch}}} \qquad \text{For members connected through fit bolts} \tag{10.15}$$

$$S_v = S_{v2} = \frac{1}{\frac{a^2}{24EI_{v,ch}} + \frac{ah_0}{12EI_{pp}}} \quad \text{For members connected preloaded bolts} \tag{10.16}$$

where,

$I_{v,ch}$ is the 2nd moment of area of one angle section about its minor axis

I_{pp} is the 2nd moment of area of the effective part of the packing plate

$$I_{pp} = \frac{\pi(B + 2t + t_p)^4 - \pi d^4}{64} \tag{10.17}$$

where,

t: is the thickness of the angle section

t_p: is the thickness of the packing plate

B: is the inside diameter of the bolt head (noted s in [3])

d: is the diameter of the hole

S_{v2} may also be applied if the design slip resistance $F_{s,Rd}$ for non-fully preloaded bolt connections is higher than the shear force to be transmitted (V_{Ed} – see (10.19)).

10.4.2 Buckling resistance in compression – flexural buckling about weak axis

The design buckling resistance of a compression member should be taken as:

$$N_{bv,Rd} = \frac{\chi_v A' f_y}{\gamma_{M1}} \tag{10.18}$$

χ_v: is the buckling reduction factor determined based on the slenderness $\bar{\lambda}_{v'}$ and buckling curve b

The relative slenderness $\bar{\lambda}_{v'}$ should be taken as:

$$\bar{\lambda}_{v'} = \sqrt{\frac{A' f_y}{N_{cr,v'}}} \tag{10.19}$$

The critical axial force $N_{cr,v'}$ not considering the influence of the shear stiffness is calculated as follows:

$$N_{cr,v'} = \frac{\pi^2 E I_{v'}}{L_{cr,v'}^2} \tag{10.20}$$

where,

$I_{v'}$:   is the 2nd moment of area of the built-up member around the weak axis

$L_{cr,v'}$:   is the buckling length of the built-up member for buckling around the weak axis

10.4.3 Resistance of the connection

The resistance of the connection should be verified according to [3] based on the shear force V_{Ed} calculated as follows:

$$V_{Ed} = \frac{1}{2}\frac{\pi}{L}\frac{a}{h_0}M_{Ed} \tag{10.21}$$

$$M_{Ed} = \frac{N_{Ed}\frac{L}{200}}{1-\frac{N_{Ed}}{N_{cr,Sv}}} \tag{10.22}$$

where,

> N_{Ed} is the axial forces in the built-up sections for the governing load case

10.4.4 Resistance to combined compression and bending

For angle members subjected to compression and bending, two checks for buckling around one or the other principal axis should be satisfied.

- strong axis check

$$\left(\frac{N_{Ed}}{\chi_u\frac{N_{Rk}}{\gamma_{M1}}} + k_{uu}\frac{M_{u,Ed}}{\chi_{LT}\frac{M_{u,Rk}}{\gamma_{M1}}}\right)^\xi + k_{uv}\frac{M_{v,Ed}}{\frac{M_{v,Rk}}{\gamma_{M1}}} \le 1 \tag{10.23}$$

- weak axis check

$$\left(\frac{N_{Ed}}{\chi_v\frac{N_{Rk}}{\gamma_{M1}}} + k_{vu}\frac{M_{u,Ed}}{\chi_{LT}\frac{M_{u,Rk}}{\gamma_{M1}}}\right)^\xi + k_{vv}\frac{M_{v,Ed}}{\frac{M_{v,Rk}}{\gamma_{M1}}} \le 1 \tag{10.24}$$

where,

> k_{ij} are the interaction factors that are provided in Table 10-1;
> ξ is a factor that considers the nonlinear interaction.

Table 10-1: Determination of kij factors

k_{ij} factors	
$k_{uu} = \dfrac{C_u}{1-\frac{N_{Ed}}{N_{cr,Sv,u}}}$	$k_{uv} = C_v$
$k_{vu} = C_u$	$k_{vv} = \dfrac{C_v}{1-\frac{N_{Ed}}{N_{cr,v}}}$
$C_u= 0{,}6+0{,}4\psi_u$	$C_v= 0{,}6+0{,}4\psi_v$
$-1 \le \psi_u=\dfrac{M_{2u}}{M_{1u}}\le 1$	$-1 \le \psi_v=\dfrac{M_{2v}}{M_{1v}}\le 1$

where,

> $N_{cr,Sv,u}$: is the critical axial force for buckling about the major-axis considering the shear stiffness as determined before
> $N_{cr,v}$: is the critical axial force for buckling about the minor-axis
> N_{Rk}:   is the characteristic value of the axial force resistance of the built-up section: Af_y
> $M_{u,Rk}$: is the characteristic value of the strong axis bending resistance of the built-up section: $0{,}9W_uf_y$
> $M_{v,Rk}$: is the characteristic value of the weak axis bending resistance of the built-up section: $0{,}9W_vf_y$
> C_u, C_v: are the equivalent uniform moment factors

χ_u, χ_v: are the reduction factors for buckling about the strong/weak axis

χ_{LT}:   is the reduction factor for lateral torsional buckling determined based on the critical moment M_{cr} and reduction curve a as follows

The ξ-factor is:

$\xi = 1,5$ for SBE members
$\xi = 1,1$ for SBU members

The critical moment M_{cr} and the slenderness $\bar{\lambda}_{LT}$ are calculated as follows:

$$\bar{\lambda}_{LT} = \sqrt{\frac{0,9 W_u f_y}{M_{cr}}} \tag{10.25}$$

$$M_{cr} = C_b \pi \frac{\sqrt{EI_v GI_t}}{L} \tag{10.26}$$

I_v is the second moment of area of the built-up member considered as integral (considering $S_v = \infty$) about its minor axis

11 Practical examples

In the present chapter, design examples of the application of the rules from Chapters 7 to 10 are given. The examples do not cover the overall design of structures or the design of connections. They are limited to the verification of individual members to explain how the new design rules are to be applied in practice.

11.1 Design of a single angle leg member of a steel lattice transmission tower

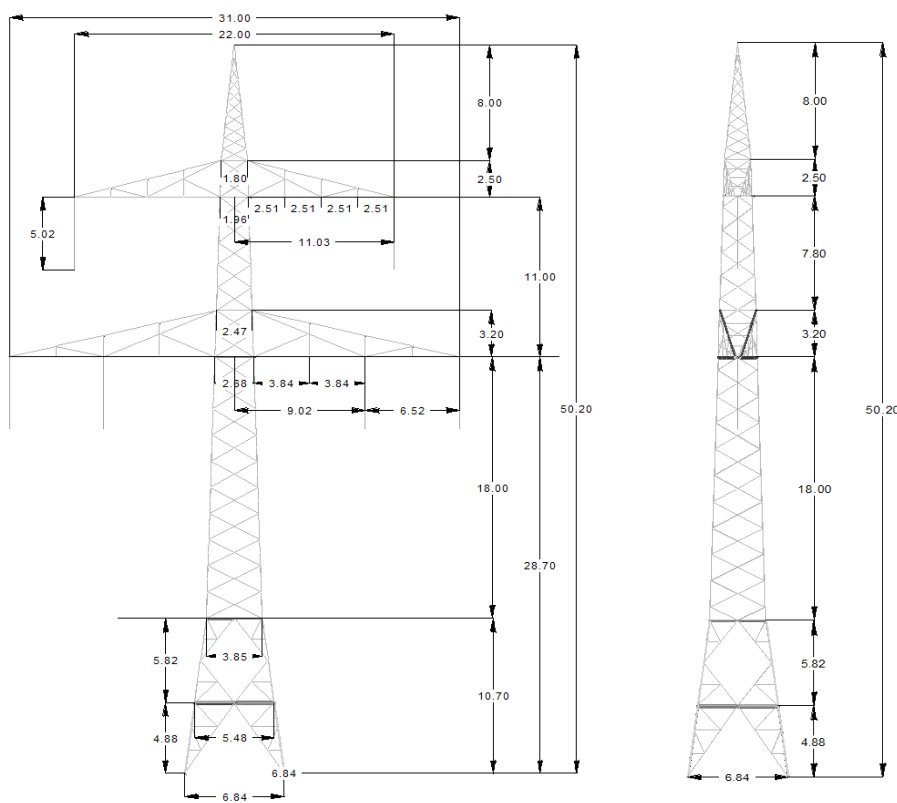The design example involves a standard Danube suspension tower with a height of 50.2m (Figure 11-1).

Figure 11-1: Dimension of the Danube tower

It is supposed that the suspension tower is part of a 380-kV transmission line with a distance between the towers of 350m. The tower is located in "the Erzgebirge" in Saxony, Germany.
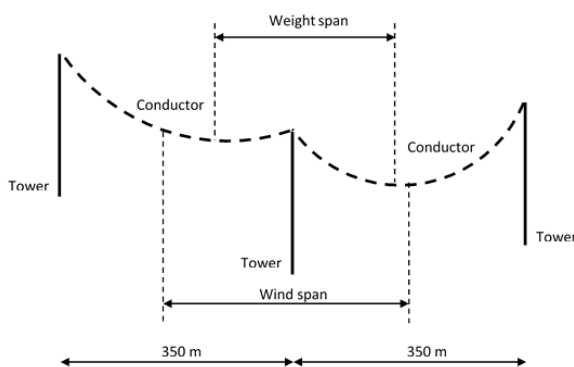

Figure 11-2: Definition of wind span and weight span

Steel grade S355J2 was selected for the leg profiles, the horizontal members of the cross arms and the primary and secondary bracing members.
The design focuses on the verification of a single leg member in the lowest segment of the tower.

A predesign of the tower structure was carried out with the software TOWER – Version 15.0. TOWER and a subsequent optimization process deliver the single equal leg angle profile L150x150x13 in S355J2 for the four legs.

The loading of the leg for the governing load combination is as follows:

- $N_{Ed} = -549,6kN$
- $M_{u,Ed} = 0,6159kNm$
- $M_{v,Ed} = -2,092kNm$ (Tip in tension)

The cross-section characteristics of the leg profile are indicated in Table 11-1:

Table 11-1: Cross section characteristics of leg members – L150x150x13

Properties		
Individual angle section	Area:	$A = 37,6cm^2$
	Thickness:	$t = 13mm$
	Radius:	$r = 16mm$
	Second moment of area about the y-and z-axes:	$I_y = I_z = 791,7cm^4$
	Second moment of area about the u-and v-axes:	$I_u = 1259cm^4$ $I_v = 324,6cm^4$
	Elastic modulus about the y-and z-axes	$W_y = W_z = 73,07cm$
	Length:	$L = 5,00m$
	Buckling length about the u-and v-axes	$L_{cr} = 1,67m$

The classification of the cross section is shown in Table 11-2:

Table 11-2: Cross section classification

Cross- section classification	
$c = h - t - r = 150 - 13 - 16 = 121mm$ $t = 13mm$ $\frac{c}{t} = 9,31$ $\varepsilon = \sqrt{\frac{235}{f_y}} = 0,81$	
Compression force N: Table 7-1	$\frac{c}{t} = 9,31 \le 13,9 \cdot \varepsilon = 11,3$ Class 2
Strong axis bending M$_u$: Table 7-1	$\frac{c}{t} = 9,31 \le 16 \cdot \varepsilon = 13,0$ Class 2
Weak axis bending M$_v$: Tip in tension Table 7-1	$\frac{c}{t} = 9,31 \le 30 \cdot \varepsilon = 24,3$ Class 2

The cross-section verifications are listed in Table 11-3:

<div align="center">Table 11-3: Cross-section verifications</div>

Cross-section verification	
Tension $N_{t,Rk}$: 7.4.1	$$N_{t,Rk} = \frac{A \cdot f_y}{\gamma_{M0}} = \frac{3760 \cdot 355}{1,0} = 1334,8kN$$ $$N_{Ed} = 549,6\ kN \ \le N_{t,Rk} = 1334,8kN$$
Compression $N_{c,Rk}$: 7.4.2	$$N_{Ed} = 549,6\ kN \ \le N_{c,Rk} = 1334,8kN$$
Strong axis bending $M_{u,Rk}$: 7.4.3	$$W_{el,u} = \frac{I_u}{0,5h\sqrt{2}} = \frac{1259}{0,5 \cdot 150 \cdot \sqrt{2}} = 118,7cm^3$$ $$W_u = \alpha_{2,u}W_{el,u} = 1,5 \cdot 118,7 = 178,05cm^3$$ $$M_{u,Rk} = W_u \frac{f_y}{\gamma_{M0}} = \frac{178,05 \cdot 355}{1,0} = 63,21kNm$$ $$M_{u,Ed} = 0.6159\ kNm \ \le\ M_{u,Rk} = 63,21kNm$$
Weak axis bending $M_{v,Rk}$: 7.4.4	$$h_1 = \frac{A}{4t} = \frac{3760}{4 \cdot 13} = 7,2cm$$ $$h_2 = h - h_1 = 15 - 7,23 = 7,8cm$$ $$\gamma_{G1} = \frac{h_1}{4} + \frac{h_2}{2} + \frac{t}{4} = \frac{7,2}{4} + \frac{7,8}{2} + \frac{1,3}{4} = 6,0cm$$ $$\gamma_{G2} = \frac{h_2^2 + h_2 t - t^2}{4h_2 - 2t} = \frac{7,8^2 + 7,8 \cdot 1,3 - 1,3^2}{4 \cdot 7,8 - 2 \cdot 1,3} = 2,4cm$$ $$C = \sqrt{2}\left(\frac{h_2}{2} - \gamma_{G2}\right) = \sqrt{2} \cdot \left(\frac{7,8}{2} - 2,4\right) = 2,1cm$$ $$d = \sqrt{2}\left(\gamma_{G1} - \frac{h_2}{2}\right) = \sqrt{2} \cdot \left(6,0 - \frac{7,8}{2}\right) = 3,0cm$$ $$W_{pl,v} = \frac{A}{2}(C + d) = \frac{37,60}{2} \cdot (2,1 + 3,0) = 96,1cm^3$$ $$M_{v,Rk} = W_{pl,v}\frac{f_y}{\gamma_{M0}} = \frac{96100 \cdot 355}{1,0} = 34,12kNm$$ $$M_{v,Ed} = 2,092\ kNm \ \le\ M_{v,Rk} = 34,12kNm$$

The buckling resistance of the leg profiles is verified in Table 11-4:

<div align="center">Table 11-4: Member verifications</div>

Buckling verifications	
Flexural buckling $N_{b,Rd}$: 7.5.1	$$N_{cr,u} = \frac{\pi^2 \cdot E \cdot I_u}{L_{cr,u}^2} = \frac{\pi \cdot 210000 \cdot 1259}{1,67^2} = 9356,5kN$$ $$N_{cr,v} = \frac{\pi^2 \cdot E \cdot I_v}{L_{cr,v}^2} = \frac{\pi \cdot 210000 \cdot 324,6}{1,67^2} = 2412,3kN$$ $$\bar{\lambda}_u = \sqrt{\frac{Af_y}{N_{cr,u}}} = \sqrt{\frac{3760 \cdot 355}{9356,5}} = 0,378$$

$$\bar{\lambda}_v = \sqrt{\frac{Af_y}{N_{cr,v}}} = \sqrt{\frac{3760 \cdot 355}{2412,3}} = 0744$$

S355J2 → Buckling curve b → $\alpha = 0,34$

$$\Phi_u = 0,5\left[1 + \alpha(\overline{\lambda_u} - 0,2) + \bar{\lambda}^2_u\right]$$
$$= 0,5[1 + 0,34(0,378 - 0,2) + 0,378^2]$$
$$= 0,602$$

$$\Phi_v = 0,5\left[1 + \alpha(\overline{\lambda_v} - 0,2) + \bar{\lambda}^2_v\right]$$
$$= 0,5[1 + 0,34(0,744 - 0,2) + 0,744^2]$$
$$= 0,869$$

$$\chi_u = \frac{1}{\Phi_u + \sqrt{\Phi_u^2 - \bar{\lambda}_u^2}} = \frac{1}{0,602 + \sqrt{0,602^2 - 0,378^2}}$$
$$= 0,934$$

$$\chi_v = \frac{1}{\Phi_v + \sqrt{\Phi_v^2 - \bar{\lambda}_v^2}} = \frac{1}{0,869 + \sqrt{0,869^2 - 0,744^2}}$$
$$= 0,760$$

$$\chi_{min} = \min(\chi_u, \chi_v) = 0,760$$

$$N_{b,Rd} = \frac{\chi_{min}A \cdot f_y}{\gamma_{M1}} = \frac{0,760 \cdot 3760 \cdot 355}{1,1} = 922,2kN$$

$$N_{Ed} = 549,6 \ kN \ \leq N_{b,Rd} = 922,2kN$$

Strong axis bending M_{u,Rd}: 7.5.2	$$C_b = \frac{12,5 \cdot M_{max}}{2,5M_{max} + 3M_A + 4M_B + 3M_C}$$ $$= \frac{12,5 \cdot 0,6159}{2,5 \cdot 0,6159 + 3 \cdot 0,210 + 4 \cdot 0,502 + 3 \cdot 0,337} = 1,48$$ $$\leq 1,50$$ $$M_{cr} = C_b \frac{0,46 \cdot E \cdot h^2 \cdot t^2}{l} = 1,48 \frac{0,46 \cdot 210000 \cdot 150^2 \cdot 13^2}{5^2}$$ $$= 108,73kNm$$ $$\bar{\lambda}_{LT} = \sqrt{\frac{W_u f_y}{M_{cr}}} = \sqrt{\frac{178050 \cdot 355}{108730000}} = 0,762$$ S355J2 → Buckling curve a → $\alpha_{LT} = 0,21$ $$\Phi_{LT} = 0,5\left[1 + \alpha_{LT}(\overline{\lambda_{LT}} - 0,2) + \bar{\lambda}^2_{LT}\right]$$ $$= 0,5[1 + 0,21(0,762 - 0,2) + 0,762^2]$$ $$= 0,85$$ $$\chi_{LT} = \frac{1}{\Phi_{LT} + \sqrt{\Phi_{LT}^2 - \bar{\lambda}_{LT}^2}} = \frac{1}{0,85 + \sqrt{0,85^2 - 0,762^2}}$$ $$= 0,815 \leq \begin{cases} 1,0 \\ \frac{1}{\bar{\lambda}_{LT}^2} = 0,857 \end{cases}$$ $$M_{u,Rd} = \chi_{LT}W_u \frac{f_y}{\gamma_{M0}} = 0,815 \frac{178,05 \cdot 355}{1,1} = 46,83kNm$$ $$M_{u,Ed} = 0,6159 \ kNm \ \leq \ M_{u,Rd} = 46,83kNm$$

Weak axis bending $M_{v,Rd}$: 7.5.3	$M_{v,Ed} = 2,092\ kNm\ \leq\ M_{v,Rk} = 34,12 kNm$
Resistance to combined compression and bending 7.5.4	$-1 \leq \psi_u = \dfrac{M_{2u}}{M_{1u}} = \dfrac{0,337}{0,616} = 0,547 \leq 1$ $-1 \leq \psi_v = \dfrac{M_{2v}}{M_{1v}} = \dfrac{0,06}{2,09} = 0,029 \leq 1$ $C_u = 0,6 + 0,4\psi_u = 0,6 + 0,4 \cdot 0,547 = 0,8$ $C_v = 0,6 + 0,4\psi_v = 0,6 + 0,4 \cdot 0,029 = 0,6$ $k_{uu} = \dfrac{C_u}{1 - \dfrac{N_{Ed}}{N_{cr,u}}} = \dfrac{0,8}{1 - \dfrac{549,6}{9356,5}} = 0,85$ $k_{vv} = \dfrac{C_v}{1 - \dfrac{N_{Ed}}{N_{cr,v}}} = \dfrac{0,6}{1 - \dfrac{549,6}{2412,3}} = 0,78$ $k_{uv} = C_v = 0,60$ $k_{vu} = C_u = 0,80$ $\dfrac{c}{t} = 9,31\ \leq 16 \cdot \varepsilon = 13,0 \to \xi = 2$ Strong axis bending: $\left(\dfrac{N_{Ed}}{N_{bu,Rd}} + k_{uu}\dfrac{M_{u,Ed}}{M_{u,Rd}}\right)^{\xi} + k_{uv}\dfrac{M_{v,Ed}}{M_{v,Rd}} \leq 1$ $\left(\dfrac{549,6}{1133,4} + 0,85\dfrac{0,6159}{46,83}\right)^{2} + 0,6\dfrac{2,092}{34,12} = 0,28 \leq 1$ Weak axis bending: $\left(\dfrac{N_{Ed}}{N_{bv,Rd}} + k_{vu}\dfrac{M_{u,Ed}}{M_{u,Rd}}\right)^{\xi} + k_{vv}\dfrac{M_{v,Ed}}{M_{v,Rd}} \leq 1$ $\left(\dfrac{549,6}{922,2} + 0,80\dfrac{0,6159}{46,83}\right)^{2} + 0,78\dfrac{2,092}{34,12} = 0,42 \leq 1$

11.2 Design of a strengthened member with CFRP

The design example involves the strengthening of a common type of a telecommunication tower with a height of 51m. In this type of tower, typical failure occurs in braces in the middle part of the tower, as shown in Figure 11-3. The conventional method of strengthening these members includes either replacing brace members with new members of larger section or adding an extra member to the existing making a new built-up member. The main disadvantage of this method is that it causes an increase in total tower's weight and also in wind loads, since the wind reference area increases. On the other hand, in the new innovative method of using FRPs to strengthen the tower's members, there is no need for new or larger sections. CFRP plates are attached to the existing members, and as a result no increase in the total weight or wind loads exists. In this example, CFRP plates are placed only externally to both legs of the existing angle section, as shown in Figure 11-3, to make the hybrid member. The properties and the resistance of the strengthened brace member are calculated based on the design rules for hybrid angle members that were previously presented in Chapter 9.
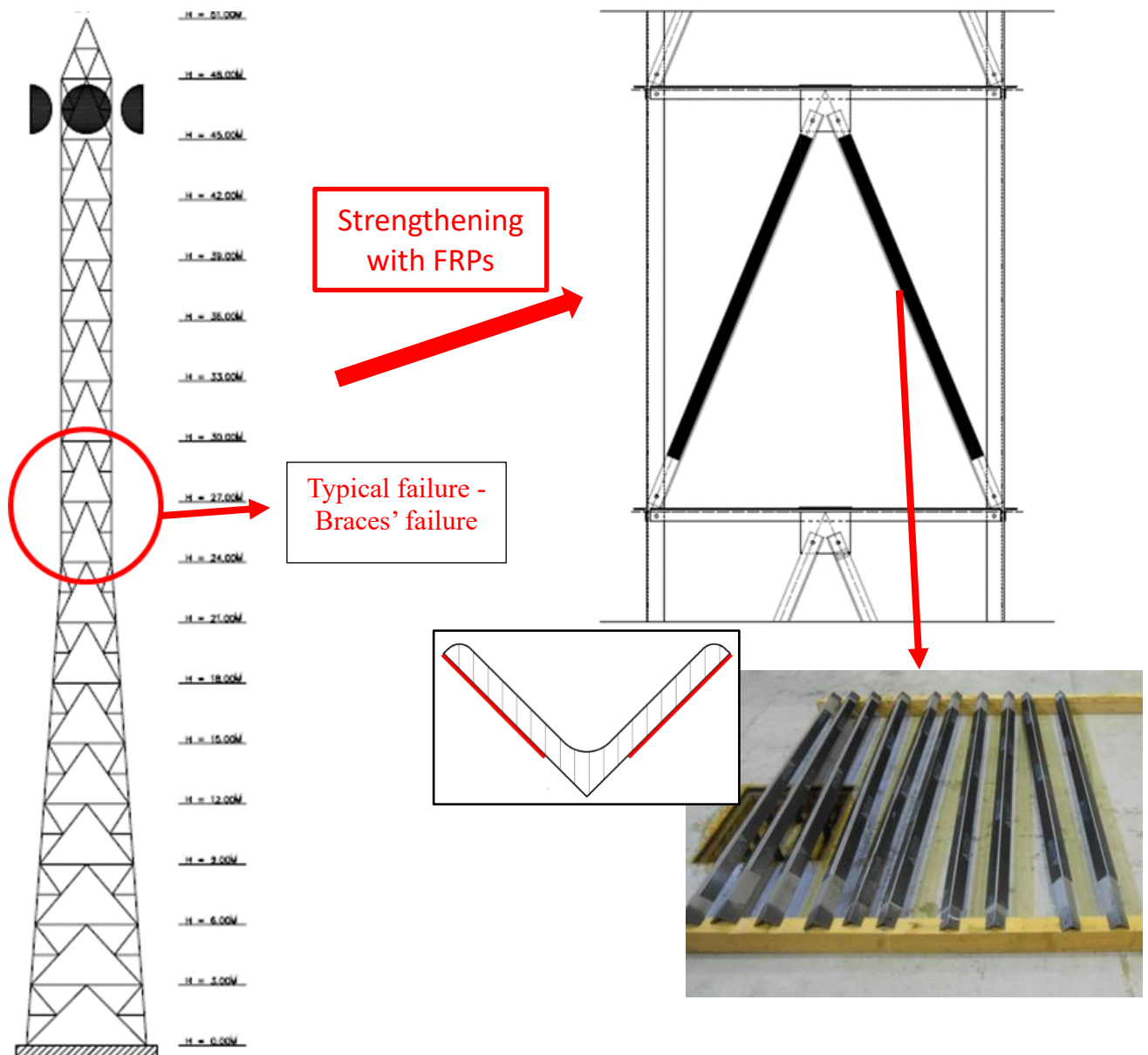
Figure 11-3: Typical telecommunication tower. Strengthening of braces using FRP plates

11.2.1 Hybrid section properties

The members that were selected to be strengthened are brace members, of equal angle section L70x70x7. CFRP plates S512, with a width of 50mm and thickness of 1,2 mm, are selected. The steel grade is S235. The material properties of both Steel and FRP material as well the mechanical properties of the steel section are presented in Table 11-5 and Table 11-6.

Table 11-5: Material properties

Material	E (GPa)	f_y (MPa)	f_u (MPa)
Steel	210	235	360
FRP	165	-	2900

<div align="center">**Table 11-6: Cross-section mechanical properties L70x70x7 (unstrengthened section)**</div>

Section	h (mm)	t_s (mm)	As (cm²)	u_{Gs} (mm)	y_{Gs} (mm)	$I_y = I_z$ (cm⁴)	I_u (cm⁴)	I_v (cm⁴)
L 70x70x7	70	7,0	9,40	27,9	19,7	42,3	67,1	17,5

| FRP 2xS512	b_f (mm)	t_f (mm)	Af (cm²)	u_{Gf} (mm)
	50	1,2	1,2	31,8

The hybrid steel-CFRP section is transformed to an entirely steel section with equivalent cross-section properties, denoted with the subscript i.

Modular ratio between steel and FRP material: $n = \frac{E_s}{E_f} = \frac{210}{165} = 1,27$

Cross-section area of equivalent section: $A_i = A_s + \frac{A_f}{n} = 9,40 + \frac{1,2}{1,27} = 10,34 cm^2$

where,

$A_f = 2 \cdot b_f \cdot t_f = 2 * 50 * 1,2 = 120 \ mm^2$ is the cross-section area of the CFRP plates
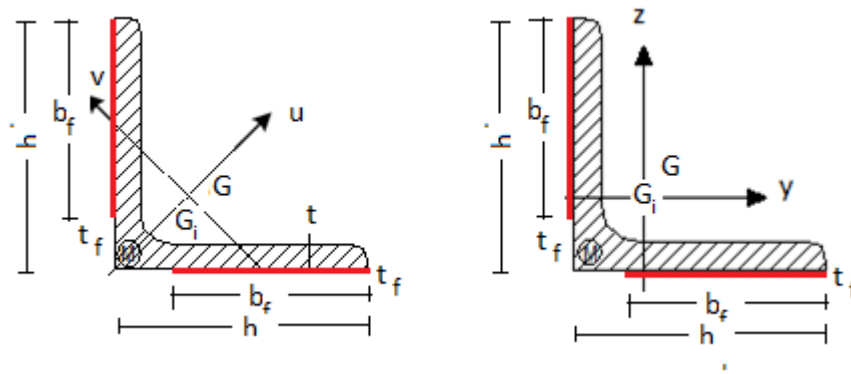
G_i centroid of hybrid section, G centroid of steel section

Figure 11-4: Notation, principal and geometric axes for hybrid section

Position of centroid

Principal axes

$v_{Gi} = 0$

$u_{Gi} = \frac{A_s \cdot u_{Gs} + A_f/n \cdot u_{Gf}}{A_i} = \frac{9,40 \cdot 2,79 + 1,2/1,27 \cdot 3,18}{10,34} = 28,3 mm$

where:

$u_{Gf} = \left(h - \frac{b_f}{2}\right)/\sqrt{2} = (70 - \frac{50}{2})/\sqrt{2} = 31,8 mm$ is the position of the centroid of the CFRP plates

Geometric axes

$y_{Gi} = z_{Gi} = u_{Gi} * \frac{\sqrt{2}}{2} = 28,3 * \frac{\sqrt{2}}{2} = 20,0 mm$

Second moments of area

Weak axis

$I_{vi} = I_{vs} + A_s \cdot (u_{Gi} - u_{Gs})^2 + \frac{A_f}{n} \cdot \left(u_{Gi} - u_{Gf}\right)^2 =$

$$= 17,5 + 9,4 * (2,83 - 2,79)^2 + \frac{1,2}{1,27} \cdot (2,83 - 3,18)^2 = 17,63 cm^4$$

Strong axis

$$I_{ui} = I_{us} + \frac{h^3 - (h - b)^3}{3 \cdot n} \cdot t_f = 67,1 + \frac{7^3 - (7 - 5)^3}{3 \cdot 1,27} \cdot 0,12 = 77,65 cm^4$$

Geometric axes

$$I_{zi} = I_{yi} = I_{ys} + A_s \cdot (y_{Gi} - y_{Gs})^2 + \frac{A_f}{2n} \cdot y_{Gi}{}^2 + \frac{A_f}{2n} \cdot \left(z_{Gi} - \left(h - \frac{b_f}{2} \right) \right)^2 =$$

$$= 42,3 + 9,40 * (2 - 1,97)^2 + \frac{1,2}{2 * 1,27} \cdot 2^2 + \frac{1,2}{2 * 1,27} \cdot \left(2 - \left(7 - \frac{5}{2} \right) \right)^2 = 47,15 cm^4$$

11.2.2 Hybrid section resistance

Separate safety factors are used for each material. For steel sections partial safety factors γ_{Mo}, γ_{M1} equal to 1.0, as provided by EN 1993-1-1, are applied. For CFRP plates, an appropriate safety factor γ_f depending on the production method and the material uncertainties, should be used. In this example, this factor is taken as equal to 1.25. For CFRP material an additional conversion factor η, is also applied. Telecommunication towers are subjected to environmental exposure. For this reason, an adequate protective covering able to counteract environmental effects is used. In this case, conversion factor η is considered equal to 1.0. Otherwise, a value of 0.85 would have been adopted.

Classification

The application of the CFRP plates probably affects the section classification. However, CFRP plates are not taken account for the classification. Therefore, classification of the hybrid section is done according to Table 7-1, which refers to rolled angle sections. Based on it, section L70x70x7 is class 2.

Tension

$$N_{t,Rd} = A_s \cdot \frac{f_y}{\gamma_{M0}} + A_f \cdot \frac{\eta \cdot f_f}{\gamma_f} = 9,40 \cdot \frac{23,5}{1,0} + 1,2 \cdot \frac{1,0 * 290}{1,25} = 499,3 kN$$

Compression

$$N_{c,Rd} = A_s \cdot \frac{f_y}{\gamma_{M1}} + A_f \cdot \frac{\eta \cdot k \cdot f_f}{\gamma_f} = 9,40 \cdot \frac{23,5}{1,0} + 1,2 \cdot \frac{1,0 * 0,5 * 290}{1,25} = 360,1 kN$$

A reduction factor k = 0,5 of the FRP strength for pure compression is adopted.

Bending
Strong axis

$$M_{u,RD} = M_{u,pl,s,Rd} + \frac{\eta \cdot f_f \cdot t_f \cdot b \cdot (2b - h)}{3\sqrt{2} \cdot \gamma_f} = \frac{24,23 * 23,5}{1,0} + \frac{1,0 \cdot 290 \cdot 0,12 \cdot 5 \cdot (2 * 5 - 7)}{3\sqrt{2} * 1,0} =$$

$$= 6,92 kNm$$

where $M_{u,pl,s,Rd}$ is the design plastic moment resistance of the steel section for strong axis bending

Weak axis

$$M_{v,Rd} = \frac{f_y \cdot t}{\sqrt{2} \cdot \gamma_{M0}} \cdot \{(h - x_0)^2 + x_0^2\} + \frac{2 \cdot \eta \cdot f_f \cdot t_f}{3 \cdot \sqrt{2} \cdot (h - x_0) \cdot \gamma_f} \left\{(h - x_0)^3 + \left[x_0 - (h - b_f)\right]^3\right\} =$$

$$= \frac{23,5 * 0,7}{\sqrt{2} * 1,0} \cdot \{(7 - 4,15)^2 + 4,15^2\} + \frac{2 * 1,0 * 290 * 0,12}{3 \cdot \sqrt{2} \cdot (7 - 4,15) \cdot 1,25} \{(7 - 4,15)^3 + [4,15 - (7 - 5)]^3\} =$$

$$= 4,47 kNm$$

where:

$$x_0 = \frac{\frac{b}{2} - \sqrt{(b/2)^2 - ac}}{a} = \frac{\frac{223.35}{2} - \sqrt{(223,35/2)^2 - 32,9 * 1589,05}}{32,9} = 4,15 cm$$

$$a = 2f_s t_s = 2 * 23,5 * 0,7 = 32,9$$
$$b = 3f_s t_s h + f_f t_f b_f = 3 * 23,5 * 0,7 * 7 + 290 * 0,12 * 5 = 519,45$$
$$c = f_s t_s h^2 - f_f t_f b_f \left(\frac{b_f}{2} - h\right) = 23,5 * 0.7 * 7^2 - 290 * 0,12 * 5 \left(\frac{5}{2} - 7\right) = 1589,05$$

11.2.3 Buckling resistance of hybrid members

Tower's braces are subjected only to axial forces. So, the verification of tension and buckling resistance of the strengthened (hybrid) members is sufficient. The calculation of buckling resistance is calculated based on EN 1993-3-1 (Annex G). In this example, secondary bracing and triangulated hip bracing exist, so braces' buckling length is considered to be the same along all axes: $L_{cr} = 1.625\ m$. Member's both ends are considered to be rigidly connected (with two bolts), so no reduction factor is applied to buckling strength ($\eta = 1.0$), according to EN 1993-3-1 Annex G.1(3).

$$N_{b,RD} = \chi * N_{c,RD}$$

Critical buckling load

$$N_{cr,u,i} = \frac{\pi^2 * E * I_{u,i}}{L_{cr,u,i}^2} = \frac{\pi^2 * 21000 * 77,65}{162,5^2} = 609,5\ kN$$

$$N_{cr,v,i} = \frac{\pi^2 * E * I_{v,i}}{L_{cr,v,i}^2} = \frac{\pi^2 * 21000 * 17,63}{162,5^2} = 138,4 kN$$

$$N_{cr,y,i} = \frac{\pi^2 * E * I_{y,i}}{L_{cr,y,i}^2} = \frac{\pi^2 * 21000 * 47,15}{162,5^2} = 370,1 kN$$

Slenderness

$$\bar{\lambda}_u = \sqrt{\frac{N_{c,R,i}}{N_{cr,u,i}}} = \sqrt{\frac{360,1}{609,5}} = 0,769$$

$$\bar{\lambda}_v = \sqrt{\frac{N_{c,R,i}}{N_{cr,v,i}}} = \sqrt{\frac{360,1}{138,4}} = 1,613$$

$$\bar{\lambda}_y = \sqrt{\frac{N_{c,R,i}}{N_{cr,y,i}}} = \sqrt{\frac{360,1}{370,1}} = 0,986$$

Reduction factors

The reduction factor χ is determined with the effective slenderness ratio $\bar{\lambda}_{eff}$ instead of $\bar{\lambda}$. Table 11-7 shows the maximum effective slenderness among all axes. Reduction factor is derived from buckling curve **b.**

<p align="center">Table 11-7: Effective slenderness along all axes</p>

Axis	u axis	v axis	y axis	Maximum
$\bar{\lambda}$	0,769	1,613	0,986	$\bar{\lambda}_{eff} = k * \bar{\lambda}$
k	1,00	0,92	1,11	**1,48**

$$\Phi = 0.5 * \left[1 + \alpha * \left(\bar{\lambda}_{eff} - 0.2\right) + \bar{\lambda}_{eff}{}^2\right] = 0,5 * \left[1 + 0,34 * (1,48 - 0,2) + 1,48^2\right] = 1,81$$

$$\chi = \frac{1}{\Phi + \sqrt{\Phi^2 - \bar{\lambda}_{eff}{}^2}} = \frac{1}{1,81 + \sqrt{1,81^2 - 1,48^2}} = \mathbf{0,35}$$

$$N_{b,RD} = \chi * N_{c,RD} = 0,35 * 360,1 = 126,0 kN$$

As it is noticed, a significant increase **(+25,2%)** of the buckling resistance of braces members is achieved.

Brace member L70.7	
$N_{t,RD}$	$N_{b,RD}$
220.8 kN	100.6 kN

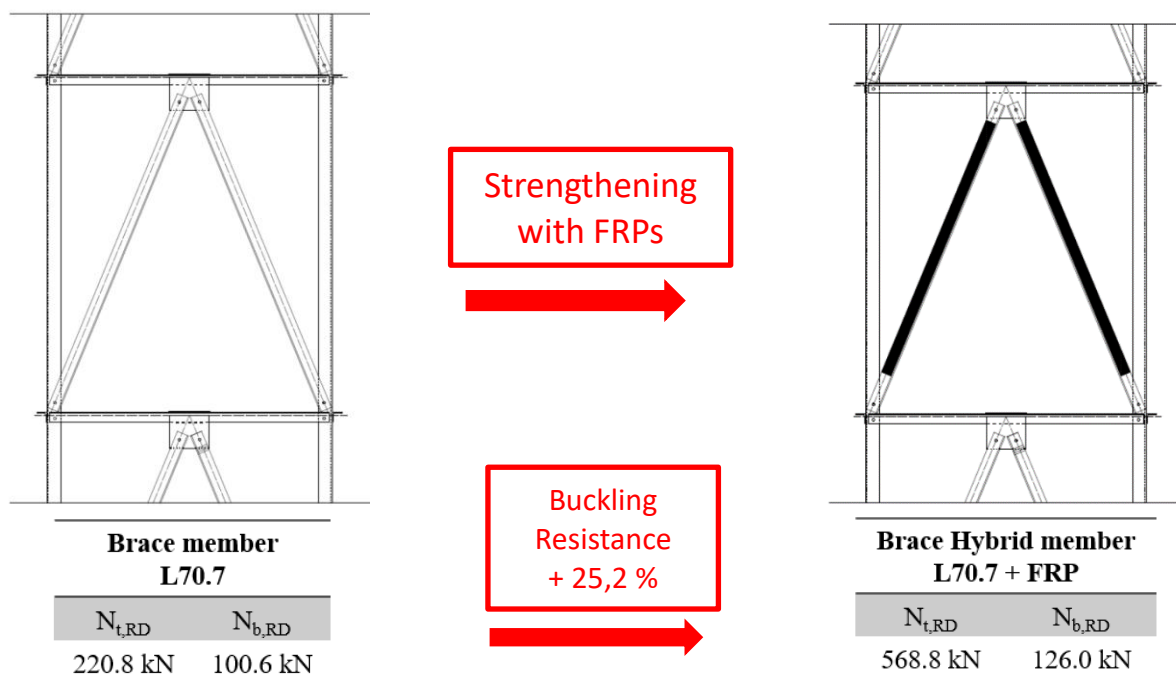| Brace Hybrid member L70.7 + FRP	
$N_{t,RD}$	$N_{b,RD}$
568.8 kN	126.0 kN

<p align="center">Figure 11-5: Resistance of brace member with and without FRP strengthening</p>

11.3 Leg-segment instability check of a steel lattice transmission tower

The electric transmission tower in 11.1 is simulated through the full non-linear finite element software FINELG [3], using beam elements. Every single member had been properly modelled, in terms of orientation and eccentricities at its extremities. Through an elastic instability analysis for a load combination $(G+W_y)$, a leg-segment instability is observed. The reference codes for the constitutive elements and the configuration of the tower leg simulated in FINELG, are illustrated in Figure 11-6, while the cross-section and the length of each member of the studied tower are reported in Table 11-8.

Table 11-8: Details of the members of the leg

Member	CS code	Cross-section	Length [m]
Diagonal 1 (left)	13	L75x75x4	6,00
Diagonal 2 (right)	13	L75x75x4	6,00
Main leg	12	L150x150x13	5,00
Horizontal level 1	4	L80x80x5	3,88
Horizontal level 1	3	L80x80x5	2,74
Horizontal level 2	46	L60x60x4	2,58
Horizontal level 2	14	L60x60x4	1,827
Horizontal level 3	46	L60x60x4	1,29
Horizontal level 3	14	L60x60x4	0,913
Bracings left or right	29	L60x60x4	2,29
Bracings left or right	28	L60x60x4	1,78
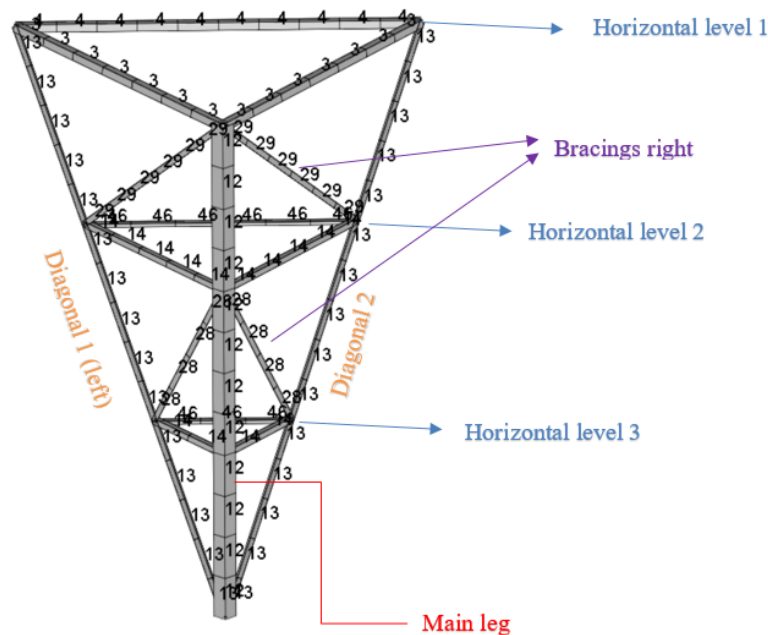
Figure 11-6: Notations of the constitutive elements of the leg of the tower

The left diagonal supports roughly 30 kN (P_1) and the right one, almost zero (P_2). The critical load multiplier obtained from FINELG is equal to $\alpha_{cr,FIN}$=**1,37**.

11.3.1 Simplified model

In the pylon, the diagonals are made of L75x75x4 angles (I_y = 314300 mm⁴) and their buckling lengths equal 6000 mm. Therefore, for the simplified model, the critical load multiplier is:

$$a_{cr,anal,1} = \frac{2\pi^2 EI_y}{L^2 \cdot (P_1 + P_2)} = \frac{2\pi^2 210000 \cdot 314300}{6000^2 \cdot (30000 + 0)} = \mathbf{1,21}$$

That is close the one obtained numerically ($\alpha_{cr,anal,1}/\alpha_{cr,FIN}$=0,881).

11.3.2 Final model

For this model, first, the torsional rigidity C of the cross-section L150x150x13 of the exterior member is calculated and it is approximately equal to:

$$C = \frac{G}{3} \cdot 2 \cdot (h - 0,5t)t^3 = \frac{80769}{3} \cdot 2 \cdot (150 - 0,5 \cdot 13)13^3 = \mathbf{1,69761 \cdot 10^{10} Nmm^2}$$

Then, the mean value of the lateral restraint R of the diagonals is:

$$R_{mean} = \frac{3C}{2L_{ext}} \cdot \frac{1}{n} \sum_{i=1}^{n} \frac{1}{d_i^2} = \frac{3 \cdot 1,69761 \cdot 10^{10}}{2 \cdot 5000} \cdot \frac{1}{2}\left(\frac{1}{913^2} + \frac{1}{1827^2}\right) = \frac{3,8177N}{mm}$$

Consequently, **$2R_{mean}=7,6354$ N/mm**, and the stiffness of the spring is:

$$K_T = \frac{4}{m^2}(2R_{mean}) = \frac{4}{3^2}(7,6354) = \mathbf{3,393} \frac{N}{mm}$$

The critical load of the equivalent column is calculated below:

$$N_{cr} = \frac{\pi^2 EI_{y,tot}}{L^2} + \frac{3}{16}K_T L = \frac{\pi^2 210000 \cdot (2 \cdot 314300)}{6000^2} \cdot 10^{-3} + \frac{3}{16}3,393 \cdot 6000 \cdot 10^{-3} = \mathbf{40,01kN}$$

And the critical load multiplier $a_{cr,anal,2}$ for the final model is equal to:

$$\boldsymbol{a_{cr,anal,2}} = \frac{N_{cr}}{P_1 + P_2} = \frac{40,01}{30 + 0} = \mathbf{1,33}$$

It is clear that this result is much closer to the one obtained numerically ($\alpha_{cr,anal,2}/\alpha_{cr,FIN} = 0,971$).

11.3.3 Ultimate resistance of the leg

The carrying capacity of the leg in compression can be roughly evaluated by the Merchant-Rankine approach (§8.2). For both models, the plastic load multiplier α_{pl} is:

$$\alpha_{pl} = \frac{2 \cdot A \cdot f_y}{P_1 + P_2} = \frac{2 \cdot 593 \cdot 345 \cdot 10 - 3}{30 + 0} = 13,639$$

By using the ratio $\alpha_{cr,anal,1}/\alpha_{pl}$, it can be seen that the leg is rather slender: $\bar{\lambda} = \sqrt{\frac{a_{pl}}{a_{cr}}} = 3,363$. With so high slenderness values, the ultimate resistance of the leg is almost equal to its critical resistance $\alpha_{u,1}=0,922\alpha_{cr,anal,1}=1,12$.

With the improved version of the design model, the slenderness slightly changes ($\bar{\lambda} = 3,198$), but the leg remains rather slender. The ultimate resistance of the leg by Merchant-Rankine, is almost equal as for the simplified model, i.e $\alpha_{u,2}=0,914\alpha_{cr,anal,2}=1,21$.

Therefore, it is very important to estimate the value of α_{cr} with high accuracy so as to minimize the "error" in the calculations.

11.4 Steel lattice girder

This last case study concerns a lattice girder fabricated from back-to-back connected angle sections with preloaded bolts. The girder is analysed through a linear elastic analysis performed with the commercial software Robot Structural Analysis. In particular, the chosen example highlights the design method that has to be applied to back-to-back connected angle sections whose packing plates are spaced by more than $15i_{min}$ and with preloaded bolts to connect the angle sections.

11.4.1 Geometry of the truss girder

The studied lattice girder, possessing a span of 20 m, corresponds to the rafter of the longitudinal portal frames of the industrial building (in black colour in Figure 11-7). The lattice girder is composed of back-to-back connected angle sections. These angle sections are connected through packing plates that possess a spacing of 50 times the minimum radius of gyration of the angles. Consequently, the built-up member cannot be treated as single member according to [2] and the effect of the shear stiffness of the connections has to be accounted for. Figure 11-7 also shows that the lower chord of the lattice girder is restrained against out-of-plane displacements at three points along the span by lacings.

The upper chord is restrained in every node of the lattice girder by the purlins (not represented in Figure 11-7).
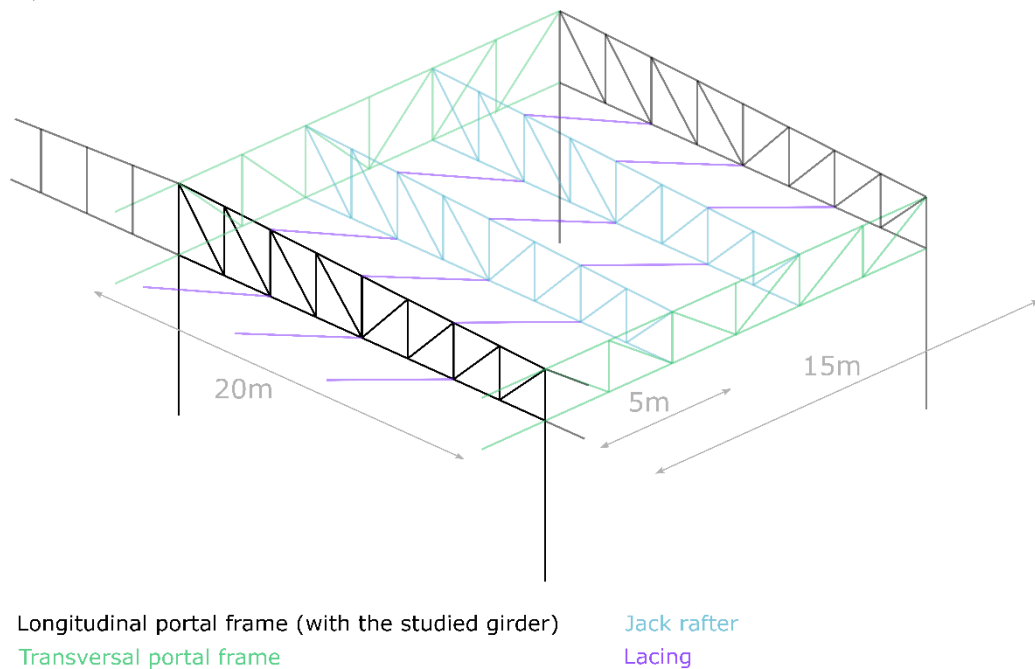

Longitudinal portal frame (with the studied girder)   Jack rafter
Transversal portal frame   Lacing

Figure 11-7: Studied lattice girder

Figure 11-8 gives a detailed view of the studied lattice girder. One may observe that three different angle sections are used depending on the position of the built-up members along the lattice girder.
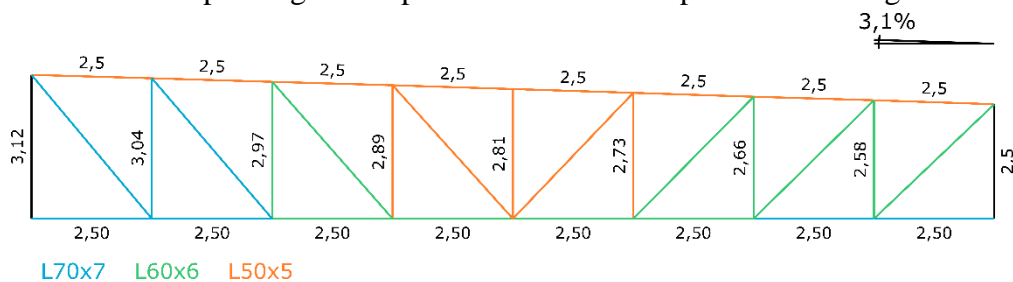

Figure 11-8: Detailed view of lattice girder

11.4.2 Materials

All elements of the lattice girder are fabricated from steel S275 JR:
- Yield strength: $f_y = 275$MPa
- Ultimate tensile strength: $f_u = 430$MPa
- Young's modulus: $E = 210\ 000$MPa
- Poisson's ratio: $\nu = 0,3$
- Density: $\rho = 7850$kg/m^3

According to [2] the yield strength f_y and the ultimate tensile strength f_u may be used for wall thicknesses that are equal to or lower than 40 mm.

11.4.3 Loads and load combinations

The studied lattice girder supports the roof of an industrial building. Consequently, it is subject to permanent loads resulting from the roof itself and the equipment. Additionally, the studied main girder transfers the climatic loads to the columns. The loads considered for the design in the following are summarised next:

Permanent loads G:

Dead load of the main girder;

Dead load of the purlins: 0,52 kN (applied to all nodes of the upper chord);

Dead load of the roof covering: 3,44 kN (applied to all nodes of the upper chord).

Live loads Q:

Electric installations: 3,75 kN (applied to all nodes of the upper chord);

Ventilation ducts: 4 kN (applied according to Figure 11-9);

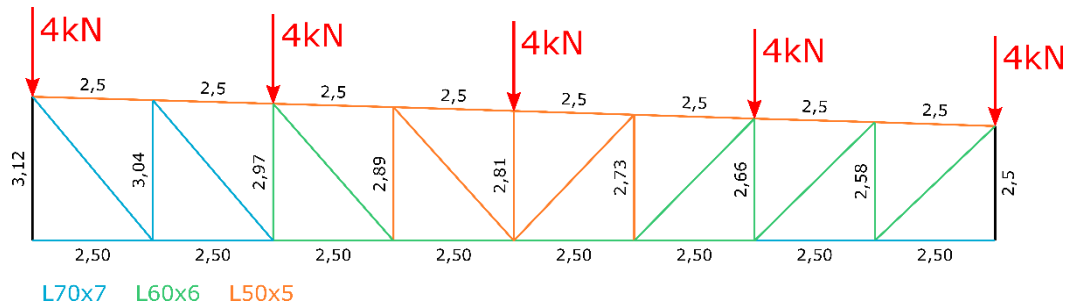Other equipment: 2,75 kN (applied to all nodes of the upper chord).

Figure 11-9: Loads resulting from ventilation ducts

Wind loads W:

Wind loads are determined according to EN 1991-1-4 [5]. The resulting loads are directly given next (the sign "-" indicates suction wind loads):

Longitudinal wind: w = -4,8 kN/m

Transversal wind: w = -4,7 kN/m

As the longitudinal wind yields the higher loads, only the value of -4,8 kN/m is considered when the internal forces are calculated.

Snow loads S:

Snow loads are determined according to EN 1991-1-3 [6] and the French National Annex. The resulting value is directly given next:

s = 3,4 kN/m

Load combinations:

The loads are combined according to EN 1990 [7]. It should be noted that all live loads Q are considered simultaneously. As the action of the wind only generates suction loads, it is not combined with snow and live loads. The following load combinations are therefore studied:

1) 1,35 G + 1,5 Q + 0,75 S
2) 1,35 G + 1,5 S + 1,05 Q
3) G + 1,5 W

11.4.4 Modelling for analyses

The lattice girder is modelled with the commercial software Robot Structural Analysis. The posts and the diagonals are considered as pinned at their ends. Inversely, the upper and lower chord are considered as continuous. In order to simplify the analysis of the lattice girder, it is extracted from the 3-dimensional numerical model of the industrial building. As the studied lattice girder corresponds to one of the intermediate spans of a multi span portal frame, its ends are considered as clamped in order to represent the effect of the continuity on the internal forces and moments. Therefore, the lattice girder is restrained at the two ends of both chords against vertical and horizontal displacements. The numerical modal of the lattice girder is represented in Figure 11-10.
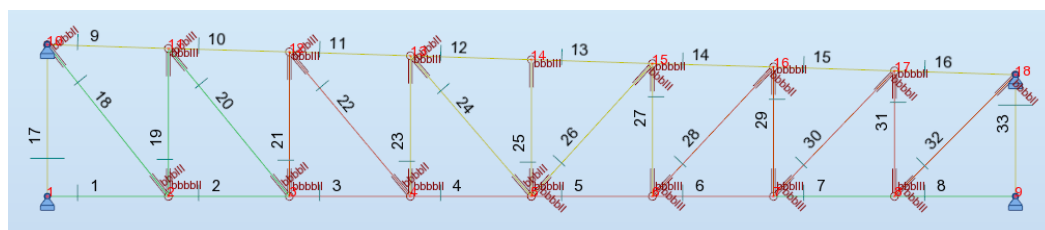
Figure 11-10: Numerical model of the lattice girder

11.4.5 Structural analysis

The internal forces are determined through first order elastic analyses of the member. Table 11-9 gives the overall maximum values of the internal axial forces. It should be noted that tension forces are considered as negative.

Table 11-9: Summary of axial forces in the members

Member	Maximum compression axial force		Maximum tension axial force	
	Combination	Force (kN)	Combination	Force (kN)
1	2	118,37	3	
2	2	36,74	3	-17,41
3	3	11,19	2	-26,6
4	3	30,22	2	-66,48
5	3	35,75	2	-77,32
6	3	20,25	2	-44,13
7	2	20,69	3	-8,64
8	2	116,04	3	-52,06
9	3	34,08	2	-77,89
10	3	6,01	2	-14,5
11	2	25,79	3	-12,5
12	2	44,55	3	-20,43
13	2	44,56	3	-19,86
14	2	36,61	3	-16,33
15	2	3,43	3	-0,28
16	3	29,2	2	-61,84
18	3	59,43	2	-130,88
19	2	101,33	3	-47,76
20	3	45,26	2	-100,05

21	2	76,2	3	-35,61
22	3	29,72	2	-62,16
23	2	46,76	3	-23,31
24	3	13,11	2	-28,81
25	2	29,63	3	-13,85
26	3	4,51	2	-11,86
27	2	34,69	3	-17,16
28	3	22,78	2	-48,66
29	2	66,21	3	-30,53
30	3	41,66	2	-93,35
31	2	94,95	3	-44,69
32	3	61,55	2	-135,06

11.4.6 Structural design

Before the structural design is performed the notations used hereafter are defined.

a   Spacing of the packing plates

b   Angle leg width

d   Bolt diameter

h_0 Distance between the angles' centroids

i_v Radius of gyration of the angle section along the minor axis (v-v)

t   Angle leg thickness

t_p Packing plate thickness

z_G Distance from the angle's centroid to the edge of the section along the z axis

A_{ch} Chord section area

B   Inside diameter of the head bolt

I_{ch} Second moment of area of an individual angle section about its z and y axes

I_{pp} Second moment of area of the packing plates

I_y Second moment of area of an individual angle about the y-y axis

$I_{y'}$ Second moment of area of the built-up member about the y'-y' axis

I_z Second moment of area of an individual angle about the z-z axis

$I_{z'}$ Second moment of area of the built-up member about the z'-z' axis

L   Total length

S_v Shear stiffness of the built-up element

The axes referred to during the structural design are defined in Figure 11-11 and Figure 11-12 for the built-up member and the individual angle section, respectively.
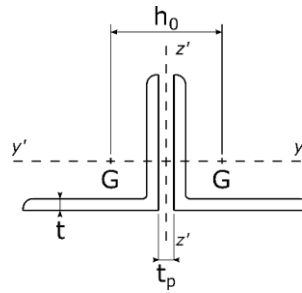
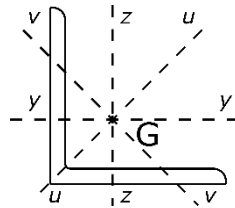**Figure 11-11: Definition of axis for the built-up member**

Figure 11-12: Definition of axis for the individual angle section

11.4.7 General

It is recalled that the spacing of the packing plates connecting the chords of the built-up member is greater than 15 times gyration of the individual angle section. According to [1], it is therefore not possible to consider the member as a single integral member. Consequently, the design procedure proposed in ANGELHY project for back-to-back angles with preloaded bolts is applied hereafter. The method is only detailed for the member marked in Figure 11-13 (noted as member 1-2 in the following). This figure also represents the restraints against out-of-plane displacements (represented as black crosses). It is recalled that the restraints result from the purlins for the upper chord and the lacings for the lower chord (see Figure 11-7).
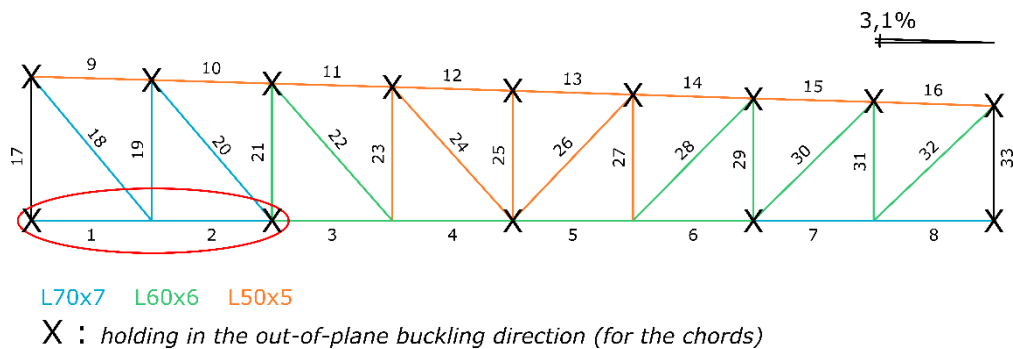
Figure 11-13: Built-up member studied explicitly

The studied member 1-2 is subjected to a stepwise constant axial force. As shown in Table 11-9, the axial force attains 118,37 kN in the first segment of the member (segment noted as 1 in Figure 11-13) whereas it attains only 36,74 kN in its second segment (segment noted as 2 in Figure 11-13). The variation of the axial force is considered for the calculation of the critical axial force for out-of-plane buckling according to the method proposed in reference [11].

11.4.8 Detailed design steps

Before the design steps are detailed, the cross-section properties of the studied member are given in Table 11-10.

Table 11-10: Cross section characteristics of member 1-2

Properties		
Individual angle section	Area:	$A_{\text{ch}} = 9,40 cm^2$
	Second moment of area about the y-and z-axes:	$I_y = I_z = I_{\text{ch}} = 42,30 cm^4$
	Distance of the angle centroid to the edge of the section along the z-axis:	$z_G = 1,97 cm$
	Packing plate thickness:	$t_p = 0,8 cm$
	Radius of gyration of the angle section along the minor axis (v-v):	$i_v = 1,36 cm$
Connection	Bolt diameter:	$d = 16 mm$
	Inside diameter of the head bolt:	$B = 26 mm$
	Second moment of area about the y-and z-axes of the packing plate:	$I_p = \dfrac{\pi(B + 2t + t_p)^4 - \pi d^4}{64} = 25,7 cm^4$
Built-up member	Area:	$A_{\text{BBE}} = 2A_{\text{ch}} = 18,80 cm^2$
	Second moment of area about the y' axis:	$I_{y'} = 2I_y = 84,60 cm^4$
	Second moment of area about the z' axis:	$I_{z'} = 2I_z + 0,5A_{\text{ch}}h_0{}^2 = 190,2 cm^4$
	Spacing of the packing plates:	$a = 50i_v = 68,0 cm$
	Distance between the angle's centroids:	$h_0 = 2z_G + t_p = 4,74 cm$

First, the resistance of member 1-2 with respect to in-plan buckling (buckling about the y'-y' axis) is checked. The member is restrained against in-plane displacements at mid-span by the post and the diagonal. Therefore, its buckling length is equal to 2,5 m. The design steps associated with in-plane buckling are summarised in Table 11-11.

Table 11-11: Design steps for in-plane buckling of the built-up member

Step	Equation	Result
Critical axial force for in-plane buckling	$N_{cr,y'} = \dfrac{\pi^2 E I_{y'}}{L_{cr,y'}{}^2}$	$N_{cr,y'} = 280,55 kN$
Relative slenderness for in-plane buckling	$\bar{\lambda}_{y'} = \sqrt{\dfrac{2A_{ch} f_y}{N_{cr,y'}}}$	$\bar{\lambda}_{y'} = 1,36$
Buckling curve	-	b: $\alpha = 0,34$
Coefficient Φ	$\Phi = 0,5\left[1 + 0,34(\bar{\lambda} - 0,2) + \bar{\lambda}^2\right]$	$\Phi = 1,62$

Reduction factor	$\chi = \dfrac{1}{\Phi + \sqrt{\Phi^2 - \bar{\lambda}^2}}$	$\chi = 0,400$
Design criterion	$\Gamma_{b,Rd} = \dfrac{N_{Ed}}{\chi\, 2A_{ch}\, f_y/\gamma_{M1}}$	$\Gamma_{b,Rd} = 0,57$

Next, the resistance of the built-up member with respect to out-of-plane instability is checked. As the distance between the packing plates ($= 50i_{min}$) exceeds the limit of $15i_{min}$ defined in [2] for the treatment of the built-up member as a whole, it is necessary to consider the effect of the shear stiffness of the connections between the chords in the design. Here, the procedure proposed in ANGELHY project for battened columns is applied (see also reference [11]). It should be noted that a distance of $50i_{min}$ between the packing plates corresponds to a practical habit in Europe.

The preparatory design steps are summarised in Table 11-12.

Table 11-12: Design steps for out-of-plane buckling of the built-up member – AngelHy formulas

Step	Equation	Result
Correction coefficient for the mid-span load (see [7])	See Sahmel abacuses [7]	$v_i = 0,53$
Effective axial force (see [7])	$N_{Ed} = P_0 + v_i P_i$	$N_{Ed} = 80,0 kN$
Critical axial force of the homogeneous built-up member	$N_{cr,1} = \dfrac{\pi^2\, E\, I_{z'}}{L_{cr,z'}{}^2}$	$N_{cr,1} = 157,7 kN$
Shear stiffness of the built-up member	$S_v = \dfrac{1}{\dfrac{ah_0}{12EI_{pp}} + \dfrac{a^2}{24EI_{ch}}}$	$S_v = 3\,746,4 kN$
Critical axial force of the built-up member	$N_{cr} = \dfrac{1}{\dfrac{1}{N_{cr,1}} + \dfrac{1}{S_v}}$	$N_{cr} = 151,3 kN$
Relative slenderness for out-plane buckling	$\bar{\lambda}_{z'} = \sqrt{\dfrac{2A_{ch}\, f_y}{N_{cr,z'}}}$	$\bar{\lambda}_{z'} = 1,85$
Buckling curve	−	$b: \alpha = 0,34$
Coefficient Φ	$\Phi = 0,5\left[1 + 0,34(\bar{\lambda} - 0,2) + \bar{\lambda}^2\right]$	$\Phi = 2,49$
Reduction factor	$\chi = \dfrac{1}{\Phi + \sqrt{\Phi^2 - \bar{\lambda}^2}}$	$\chi = 0,241$
Design criterion	$\Gamma_{b,Rd} = \dfrac{N_{Ed}}{\chi\, 2A_{ch}\, f_y/\gamma_{M1}}$	$\Gamma_{b,Rd} = 0,643$

The chosen member satisfies all design criteria. The design steps for the other members are not detailed hereafter. Rather, a synthesis of the most critical design criteria is provided in the next paragraph.

11.4.9 Synthesis of design checks

Last, Table 11-13 summarises the results of the design checks for all members. On may note, that only the most critical design criterion is specified. The notations used in Table 11-13 are recalled hereafter:

- $\Gamma_{b,y'}$: In-plane buckling of the built-up (y'-axis).
- $\Gamma_{b,y'}$: Out-of-plane buckling of the built-up (z'-axis).

Table 11-13: Synthesis of design checks

Member	$N_{Ed,max}$ (kN)	Member length (m)	Cross section	Packing plate thickness (mm)	Resistance criterion	
1	118,37	2,50	L70x70x7	8	$\Gamma_{b,z'} =$	0,64
2	36,74	2,50				
3	11,19	2,50	L60x60x6	8	$\Gamma_{b,z'} =$	0,29
4	30,22	2,50				
5	35,75	2,50	L60x60x6	8	$\Gamma_{b,z'} =$	0,39
6	20,25	2,50				
7	20,69	2,50	L70x70x7	8	$\Gamma_{b,z'} =$	0,57
8	116,04	2,50				
9	34,08	2,50	L50x50x5	8	$\Gamma_{b,y'} =$	0,57
10	6,01	2,50	L50x50x5	8	$\Gamma_{b,y'} =$	0,10
11	25,79	2,50	L50x50x5	8	$\Gamma_{b,y'} =$	0,43
12	44,55	2,50	L50x50x5	8	$\Gamma_{b,y'} =$	0,74
13	44,56	2,50	L50x50x5	8	$\Gamma_{b,y'} =$	0,74
14	36,61	2,50	L50x50x5	8	$\Gamma_{b,y'} =$	0,61
15	3,43	2,50	L50x50x5	8	$\Gamma_{b,y'} =$	0,06
16	29,20	2,50	L50x50x5	8	$\Gamma_{b,y'} =$	0,48
18	59,43	4,00	L70x70x7	8	$\Gamma_{b,y'} =$	0,64
19	101,33	3,04	L70x70x7	8	$\Gamma_{b,y'} =$	0,67
20	45,26	3,94	L70x70x7	8	$\Gamma_{b,y'} =$	0,47
21	76,20	2,97	L60x60x6	8	$\Gamma_{b,y'} =$	0,86
22	29,72	3,88	L60x60x6	8	$\Gamma_{b,y'} =$	0,54
23	46,76	2,89	L50x50x5	8	$\Gamma_{b,y'} =$	1,00
24	13,11	3,82	L50x50x5	8	$\Gamma_{b,y'} =$	0,47
25	29,63	2,81	L50x50x5	8	$\Gamma_{b,y'} =$	0,61
26	4,51	3,70	L50x50x5	8	$\Gamma_{b,y'} =$	0,15
27	34,69	2,73	L50x50x5	8	$\Gamma_{b,y'} =$	0,67

28	22,78	3,65	L60x60x6	8	$\Gamma_{b,y'} =$	0,37
29	66,21	2,66	L60x60x6	8	$\Gamma_{b,y'} =$	0,62
30	41,66	3,59	L60x60x6	8	$\Gamma_{b,y'} =$	0,66
31	94,95	2,58	L60x60x6	8	$\Gamma_{b,y'} =$	0,84
32	61,55	3,53	L60x60x6	8	$\Gamma_{b,y'} =$	0,95

12 References

[1] prEN1993-1-1: Design of steel structures - Part 1-1: General rules and rules for buildings, Brussels, Comité Européen de Normalisation (CEN), 2019.

[2] EN1993-1-1: Design of steel structures - Part 1-1: General rules and rules for buildings, Brussels, Comité Européen de Normalisation (CEN), 2005.

[3] EN 14399: High-strength structural bolting assemblies for preloading, , Brussels, Comité Européen de Normalisation (CEN), 2015.

[4] EN 1993-8: Design of steel structures - Part 1-8: Design of joints, Brussels, Comité Européen de Normalisation (CEN), 2005.

[5] EN 1991-1-4 : Actions on structures - Part 1-4: General actions; Wind actions, Brussels, Comité Européen de Normalisation (CEN), 2005.

[6] EN 1991-1-3 : Actions on structures - Part 1-4: General actions; Snow loads, Brussels, Comité Européen de Normalisation (CEN), 2004.

[7] EN 1990 : Basis of structural design, Brussels, Comité Européen de Normalisation (CEN), 2002.

[8] Delesques, R., (1972). Flambement des barres dont l'effort normal varie sur la longueur. Construction Métallique (CTICM), 4.

List of Figures

List of Tables